DEPARTMENT OF COMMERCE
FREDERICK H. MUELLER, Secretary

WEATHER BUREAU
F. W. REICHELDERFER, Chief

MONTHLY WEATHER REVIEW

JAMES E. CASKEY, JR., Editor

Volume 88
Number 3

MARCH 1960

Closed May 15, 1960
Issued June 15, 1960

CLOUD PICTURES FROM SATELLITE TIROS I*

S. FRITZ AND H. WEXLER

U.S. Weather Bureau, Washington, D.C.

Manuscript received April 29, 1960; revised May 5, 1960]

ABSTRACT

Some of the more striking examples of cloud phenomena revealed by the first pictures that have come from the experimental weather satellite, TIROS I, are presented, and broad-scale patterns in the pictures are interpreted in terms of general features of the associated weather maps. These preliminary results show that a vast variety of scales appear in the cloud patterns associated with cyclonic vortices. Marked differences, as well as similarities, in cloud patterns associated with several types of cyclones are pointed out; the cyclones discussed include mature vortices in the Atlantic and Pacific Oceans, younger cyclones over and near the United States, and a typhoon in the South Pacific Ocean. The cloud cover over an extensive area is portrayed by means of preliminary mosaics of TIROS pictures and by a schematic cloud map made from the pictures.

1. INTRODUCTION

TIROS I, an experimental weather satellite (c.f. [1]) containing two television cameras was launched on April 1, 1960, by the National Aeronautics and Space Administration. The characteristics of the satellite, its cameras, and its orbit have been reported elsewhere [2]. By April 22, it had made about 300 orbits (apogee 461.3 stat. mi.; perigee 436.0 stat. mi.; inclination 48.4°; period 99.24 min.) and its cameras had taken about 6,000 pictures of various cloud formations. The purpose of this preliminary note is to present a few examples of these cloud pictures and to show their relation to observed weather patterns.

From among these first pictures that have come from TIROS some of the more striking examples have been selected. These have been put together in two ways. The first category portrays the large-scale vortex or cyclonic storm, several hundred miles in diameter. Pictures of seven individual vortices have been selected and their relationships to features of sea level weather maps are discussed. The location of the satellite in its orbit and the direction of view of its cameras at the time of each picture have not yet been determined precisely. However, approximate locations and directions that will serve the purpose of this preliminary report are indicated on the maps.

The second category is a composite array. One array consists of two mosaics of about 30 different prints and extends from a region about 800 miles west of Ireland to the Near East. Another array, in the form of a schematic representation of clouds, extends from the Pacific coast of the United States eastward over the Mediterranean to the Near East.

2. CLOUD PATTERNS OF CYCLONIC STORMS

The first category, figures 1–8, contains seven different examples of vortices observed by TIROS in both the Northern and Southern Hemispheres. With each picture, except figures 7 and 8, is shown the weather map associated with the vortex. The weather analyses were copied from the sea level maps of the National Weather Analysis Center, U.S. Weather Bureau, Suitland, Md.

Figure 1 shows the storm that was picked up in the

*This work has been supported by the National Aeronautics and Space Administration.

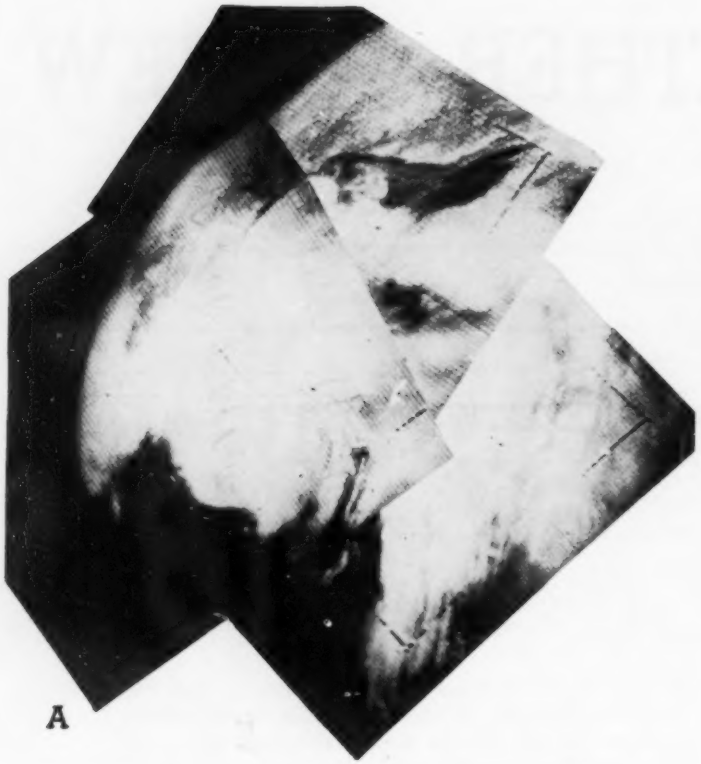

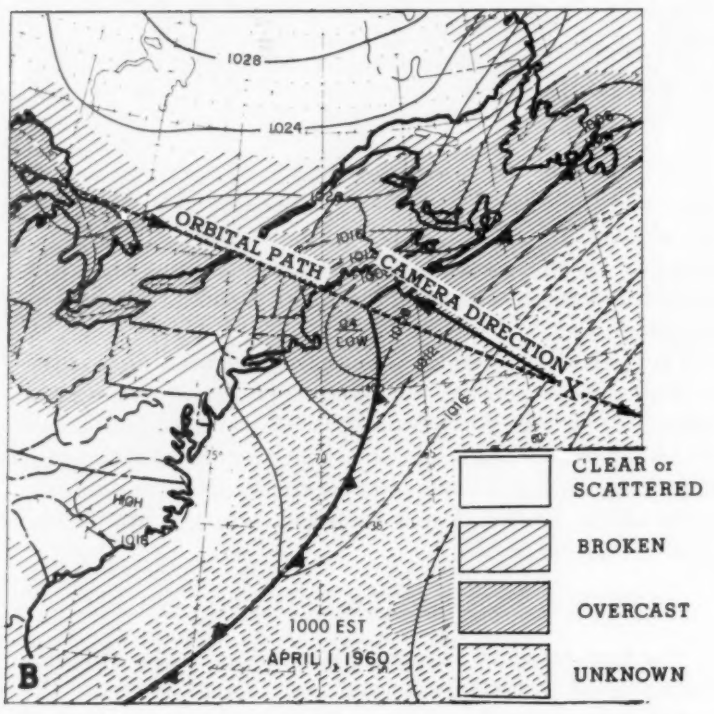

FIGURE 1.—(A) Three overlapping TIROS pictures showing extratropical cyclone centered about 120 miles east of Cape Cod, April 1, 1960. (B) Sea level weather map, 1000 EST, April 1, 1960. Point X denotes approximate location of satellite and the arrow indicates camera direction when pictures were taken.

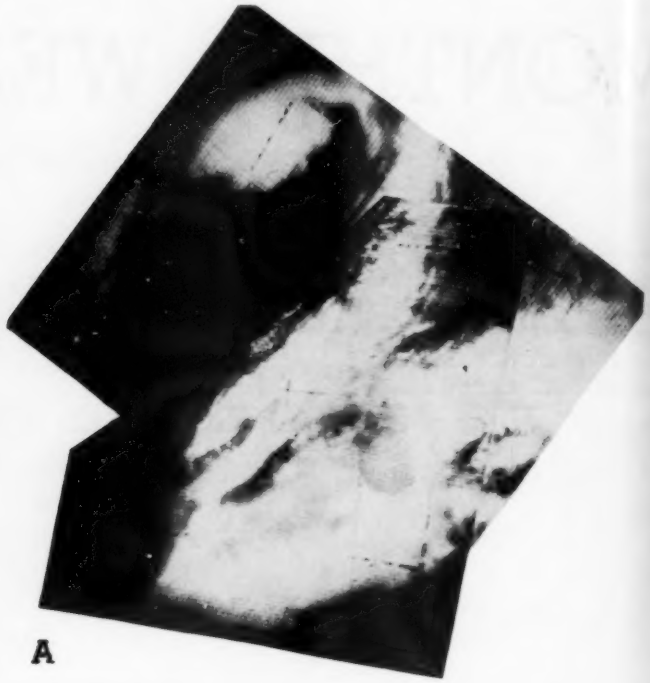

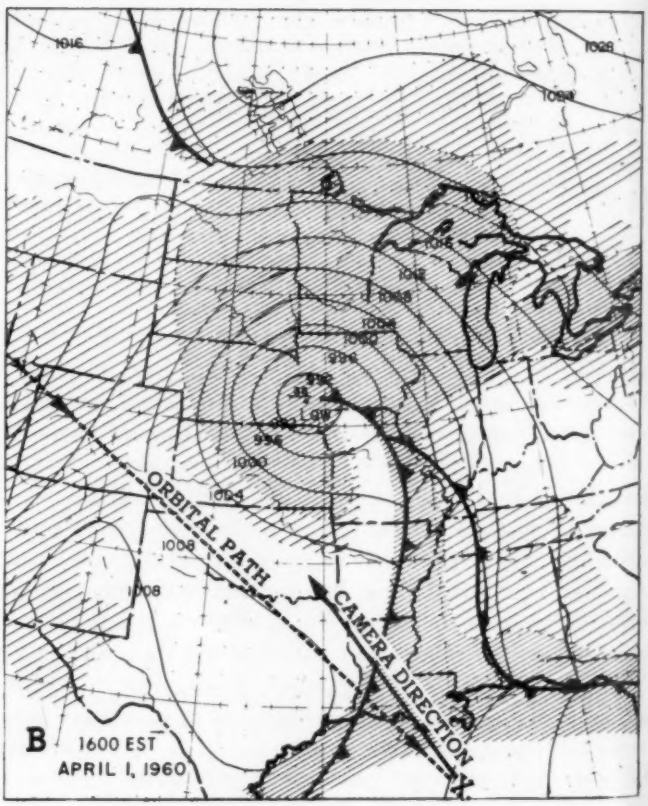

FIGURE 2.—(A) Two overlapping TIROS pictures showing extratropical cyclone centered over southeastern Nebraska, April 1, 1960. (B) Sea level weather map, 1600 EST, April 1, 1960. The key to the cloud cover analysis is given in figure 1B.

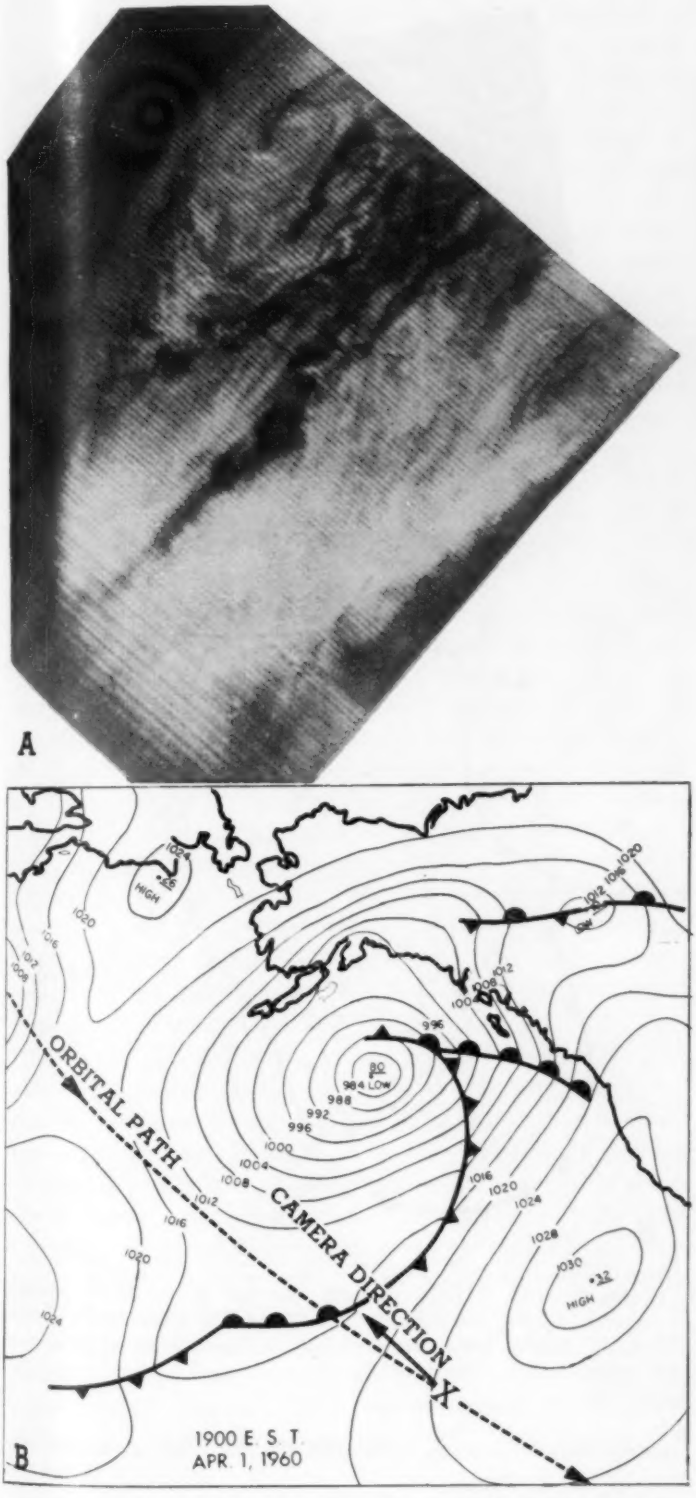

FIGURE 3.—(A) TIROS picture showing extratropical cyclone centered in the Gulf of Alaska about 500 miles southeast of Kodiak Island, April 1, 1960. (B) Sea level weather map, 1900 EST, April 1, 1960.

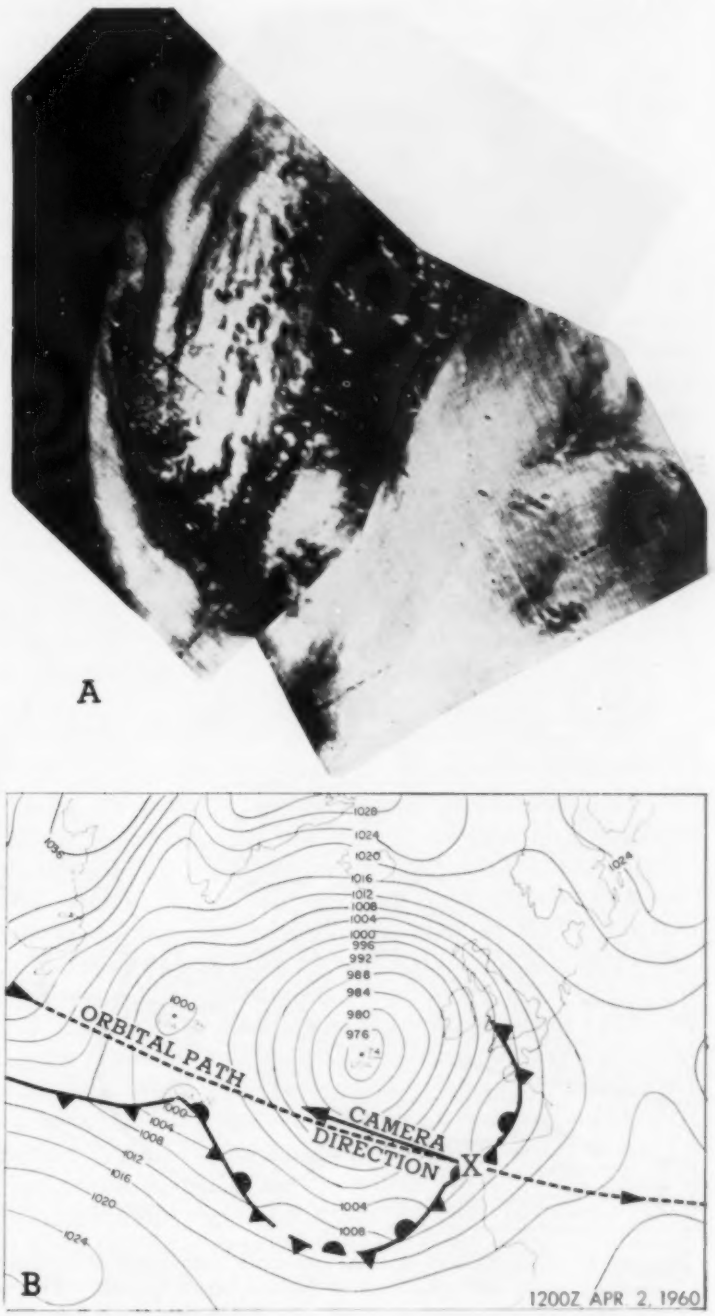

FIGURE 4.—(A) Two overlapping TIROS pictures showing extratropical cyclone centered about 400 miles west of Ireland, April 2, 1960. (B) Sea level weather map, 1200 GMT, April 2, 1960.

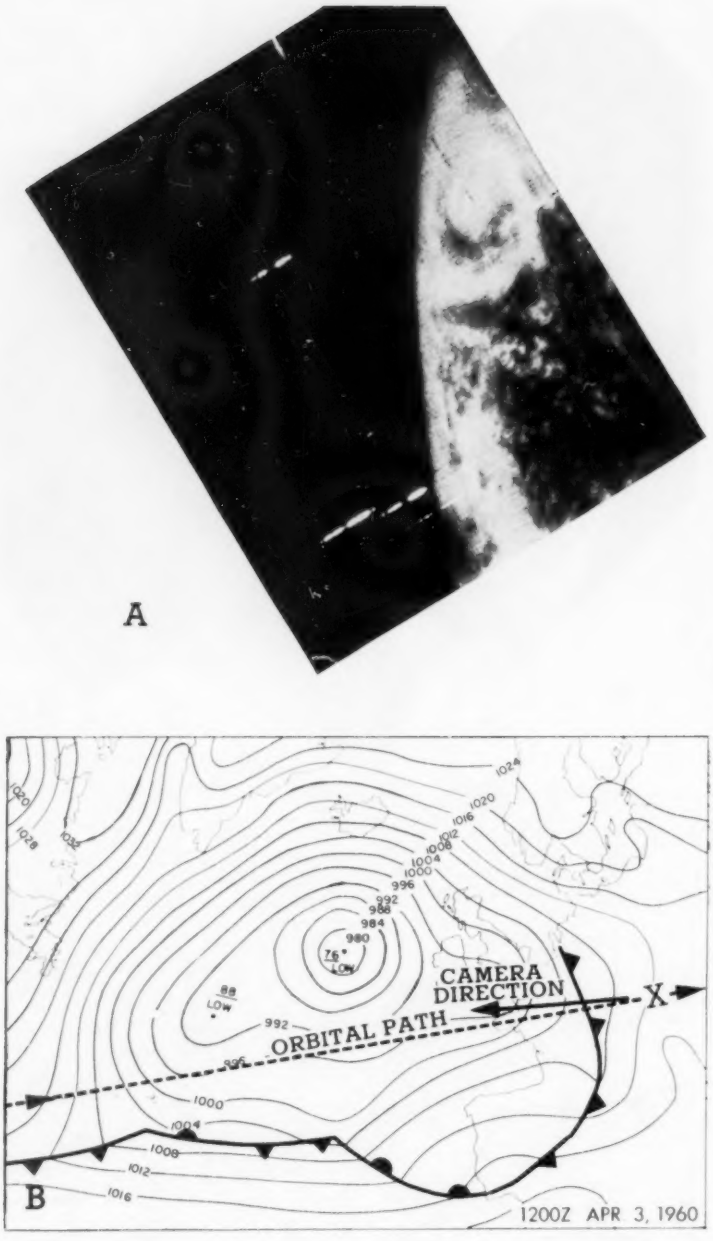

FIGURE 5.—(A) TIROS picture showing extratropical cyclone centered about 400 miles west of Ireland, April 3, 1960. This is the same storm pictured in figure 4A a day earlier. (B) Sea level weather map, 1200 GMT, April 3, 1960.

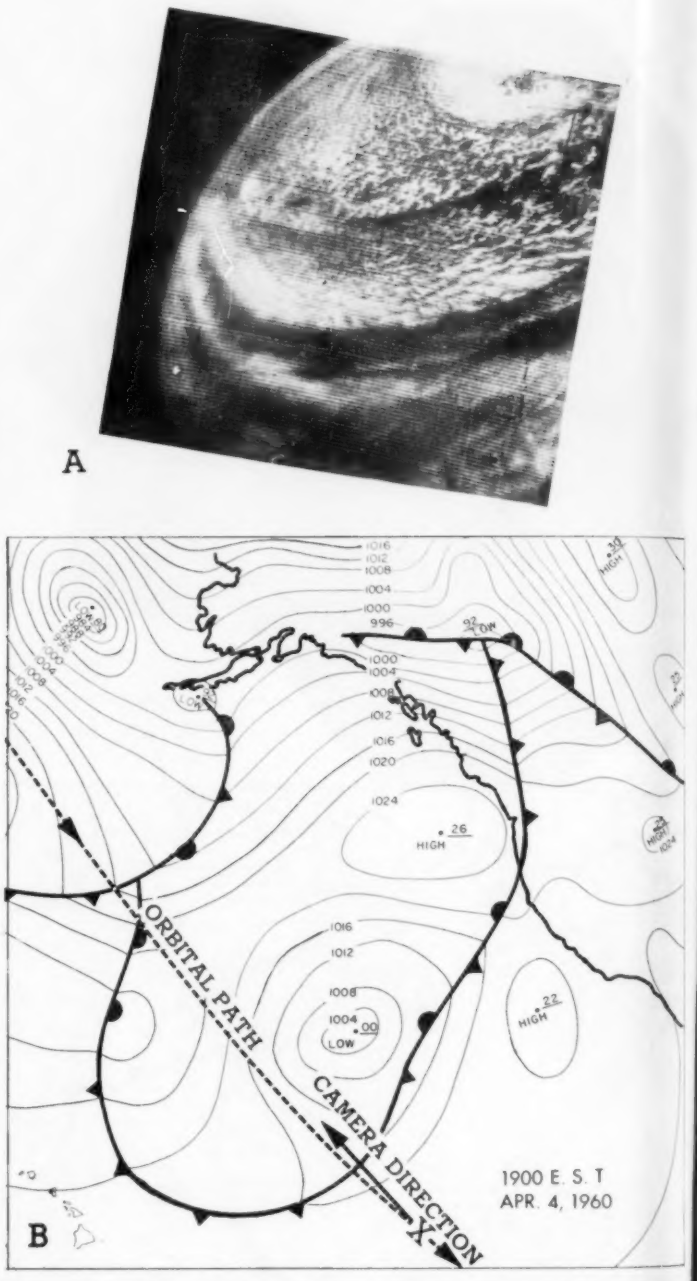

FIGURE 6.—(A) TIROS picture showing extratropical cyclone centered about 800 miles west of southern California, April 4, 1960. (B) Sea level weather map, 1900 EST, April 4, 1960.

early orbits of TIROS on the first day, April 1. The storm was centered 120 miles east of Cape Cod with continental air streaming off the east coast, and moist air over the ocean flowing northward, counterclockwise around the center, producing widespread clouds and precipitation as far north as the Gulf of St. Lawrence. Much of the Gulf of St. Lawrence and the St. Lawrence River was nearly cloudless as is indicated by the dark area near the top of the pictures.

Figure 2 shows a storm in midwestern United States that was also televised on April 1. This rather extensive storm was centered over southeastern Nebraska. Again, we see the clear, cold, dry air (represented by the dark area which is the ground underneath) moving in behind a cold

front. To the east of the front the moist air from the Gulf of Mexico is flowing into the storm center and producing rather widespread cloudiness, shown by the circular cloud near the top of the picture. Near the Gulf of Mexico, where very bright portions of the picture suggest that the clouds are very high, thunderstorms occurred.

Figure 3 shows a third vortex that was observed, also on April 1, in the Gulf of Alaska 500 miles southeast of Kodiak Island. The vortex circulation is clearly portrayed by the clouds which form a spiral array.

The associated weather map of the cyclone is based upon relatively few reports over an area which is larger than the United States; there is therefore opportunity for error because of lack of observations. The paucity of data is even more pronounced in the upper air. In these areas particularly, satellite observations similar to figure 3 will be useful in synoptic scale weather analysis as well as research.

Figure 4 shows a large, mature, occluded cyclone, about 1,000 miles in diameter, centered about 400 miles west of Ireland on April 2. The rather well-marked banded structure of the clouds of this ocean storm is quite different from the more uniform structure of clouds associated with continental and coastal storms whose cold fronts are followed by dry continental air (figs. 1 and 2). The storms over the oceans that TIROS has so far revealed seem to show more of a banded structure; the bands, ranging in width from a few miles to a few hundred miles, appear to spiral cyclonically around the storm center.

Figure 5, showing the same storm west of Ireland a day later, April 3, was photographed from a point farther to the southeast. From this view, in which the storm is near the horizon, there seems to be just one very large band winding around the center. Photogrammetric measurements may reveal the nature of the change in cloud pattern from April 2 to April 3.

Figures 6 and 7 show a cyclone located about 800 miles west of southern California on April 4 in an area where anticyclones are usually found. The storm has a cloud vortex about 1,000 miles in diameter. The cloud picture contains several scales of superimposed bands: first, a series of wide bands in which the clouds seem to start abruptly at a narrow clear zone, sometimes increasing in brightness with distance from the vortex center, only to end abruptly again in a clear zone; second, the individual bands composed of a series of smaller elements, and probably if the resolution were fine enough, there would be smaller elements within those. These are examples of the vast variety of scale of streakiness that characterizes the atmosphere.

The weather map (fig. 6B) associated with this cyclone is based on a few ship reports in the area between Hawaii and California, whereas the TIROS picture (fig. 7) reveals considerably detailed structure of the storm.

Figure 8 shows a vortex in the Southern Hemisphere, where cyclones rotate clockwise instead of counterclockwise. On April 10, this storm was located about 300 miles north of the northern tip of New Zealand. Note the dark, cloudless eye of the storm. The eye and spiral cloud bands of tropical cyclones, such as hurricanes and typhoons, have been studied by means of radar and aircraft photographs, but figure 8 shows the first single picture of a nearly complete typhoon structure as seen from high levels.

The existence of this tropical storm was known to meteorologists in the Southern Hemisphere for several days before TIROS televised it on April 10; after a message was received indicating that a storm was there, the satellite was then programmed to observe it. (TIROS can store pictures taken during only a 16-minute interval; therefore, whenever possible, it is programmed to take pictures of interesting meteorological areas on the daylight side of the earth.) This is one of several pictures taken about 0300 GMT, April 10.

The vortices that have been shown in this section are examples of the most striking phenomena that TIROS has revealed so far. It will now be necessary to study the hydrodynamics and thermodynamics which produce such cloud patterns, to acquire a greater understanding of atmospheric processes, which will then lead to a better interpretation of the cloud pictures.

3. CLOUD PATTERNS OVER EXTENDED AREAS

The second category of cloud information, shown in figures 9 and 10, is the cloud cover and patterns over an extensive area having dimensions far greater than those represented in the individual pictures shown in the preceding section. This different type of cloud information is obtained by overlapping a series of TIROS pictures to make a mosaic (fig. 9) and by deriving a schematic cloud map (fig. 10) from the pictures.

Figure 9 is a mosaic of about 30 pictures taken on orbits 14 and 15 as the satellite moved toward the southeast on April 2. The pictures start about 800 miles west of Ireland to the west of the vortex that was mentioned earlier (fig. 4). On orbit 14, a picture of the vortex was taken and 100 minutes later on orbit 15 another picture of the same storm was taken. The same cloud details can be recognized over the 100-minute interval. The mosaic gives a geographical coverage of cloud patterns beginning in the Atlantic Ocean. They include the vortex west of Ireland and show the extensive cloud area over western Europe, a massive cloud over the Swiss Alps, a general cloud area over Turkey, and a clear area in the Near East, Israel, Egypt, and North Africa.

Figure 10, based on pictures from orbits 28 and 32, on April 3, is a preliminary schematic representation of clouds over an area extending from the west coast of the United States into the Atlantic Ocean, and then from the mid-Atlantic and Europe to the Near East. Selected photographs, from which the schematic array was made, are displayed along the boundaries of the photographed area.

FIGURE 7.—Enlarged TIROS picture of the extratropical cyclone shown in figure 6. Notice the variety of scales shown by cloud patterns.

Some features of the mosaic in figure 9 on the previous day can be seen, as for example the vortex west of Ireland.

4. SUMMARY

TIROS has revealed a large degree of organization in the cloud systems over much of the earth's surface. The most striking patterns are the spiral cloud formations associated with large storms, some as much as 1,500 miles in diameter, observed in such places as the United States, North Atlantic Ocean, North and South Pacific Oceans, and the Indian Ocean (not shown here).

It is well known from radar observations that hurricanes are characterized by bands of clouds which spiral inward around a storm center. Although some suggestions have been made that extratropical cyclones also contain bands, over oceans, now as a direct result of TIROS, we see that the spiral banded cloud structure also exists around well-developed extratropical storms. Compare, for example, figures 7 and 8. In these storms the bands are separated by clear areas and range in width from several miles to a few hundred miles. Also the storm 400 miles west of Ireland (fig. 5), which is not a tropical storm, can be compared with the tropical storm north of New Zealand (fig. 8). In both cases, the cloud bands revealed the circular wind flow around the storm's center. But one of the sig-

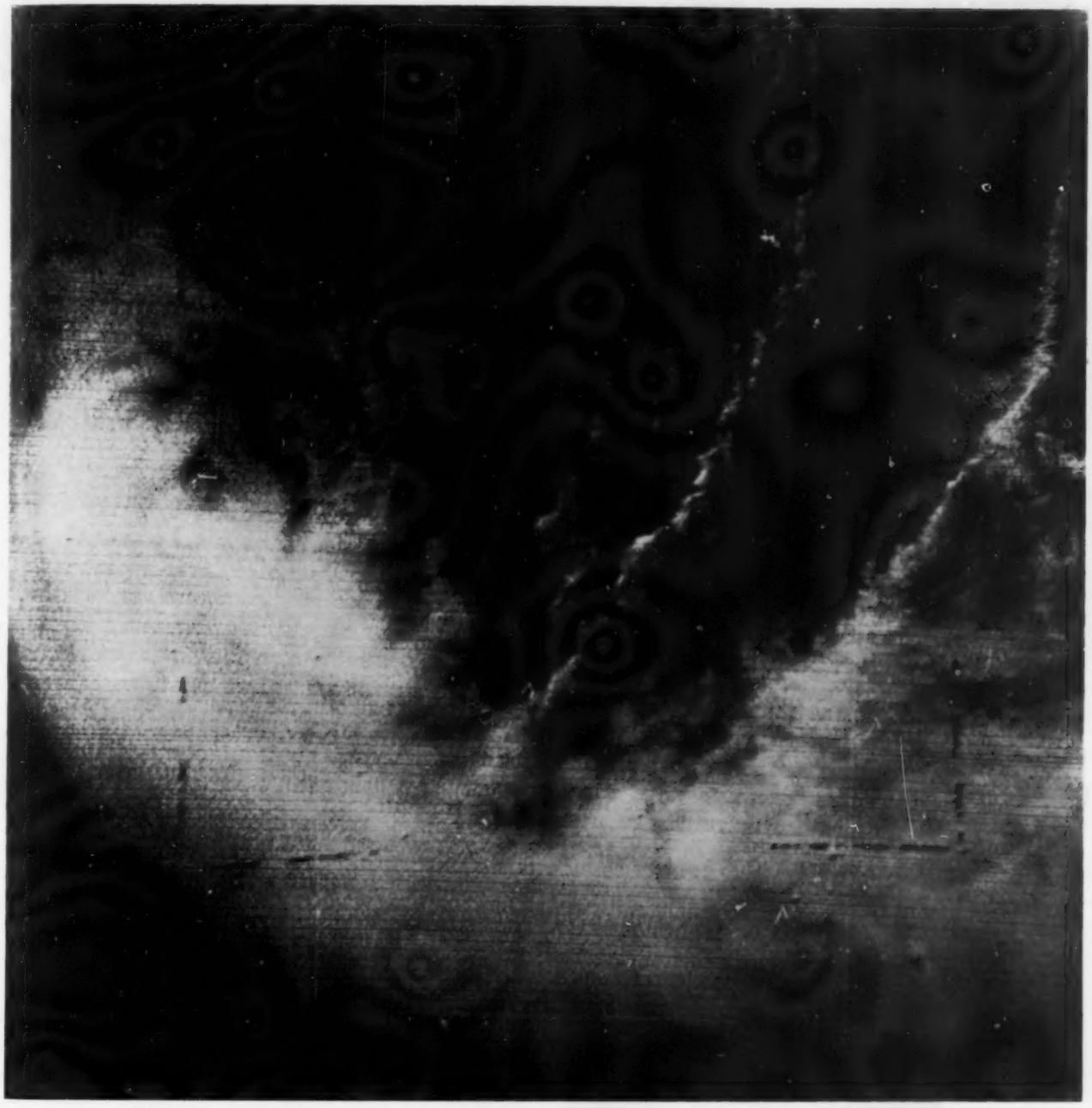

FIGURE 8.—TIROS picture of tropical cyclone centered north of New Zealand, April 10, 1960.

nificant results from TIROS is the clear indication that although storms have similarities, there may also be very marked differences. Study of the causes for these differences should reveal much about atmospheric processes and structures.

Thus far, storms observed over continents have not exhibited such fine banded structure as those over oceans. The continental storms have been associated with general cloud areas with the spaces between the bands either poorly defined or non-existent but the spiral nature of the storm was indicated more by the presence of a wedge of dry, cloudless air curving in toward the storm center behind a cold front, as shown by the Midwest storm of April 1 (fig. 2). A storm photographed on the east coast of the United States on the same day also showed this clearly (fig. 1). It had a similar cloud system without the marked banded structure. However, we do see again the cold cloudless air flowing in behind the cold front. Moreover, both of these storms contained frontal systems.

The photographs shown here are but a few of the more striking examples of cloud pictures revealed by TIROS. A systematic inspection of these cloud pictures is just

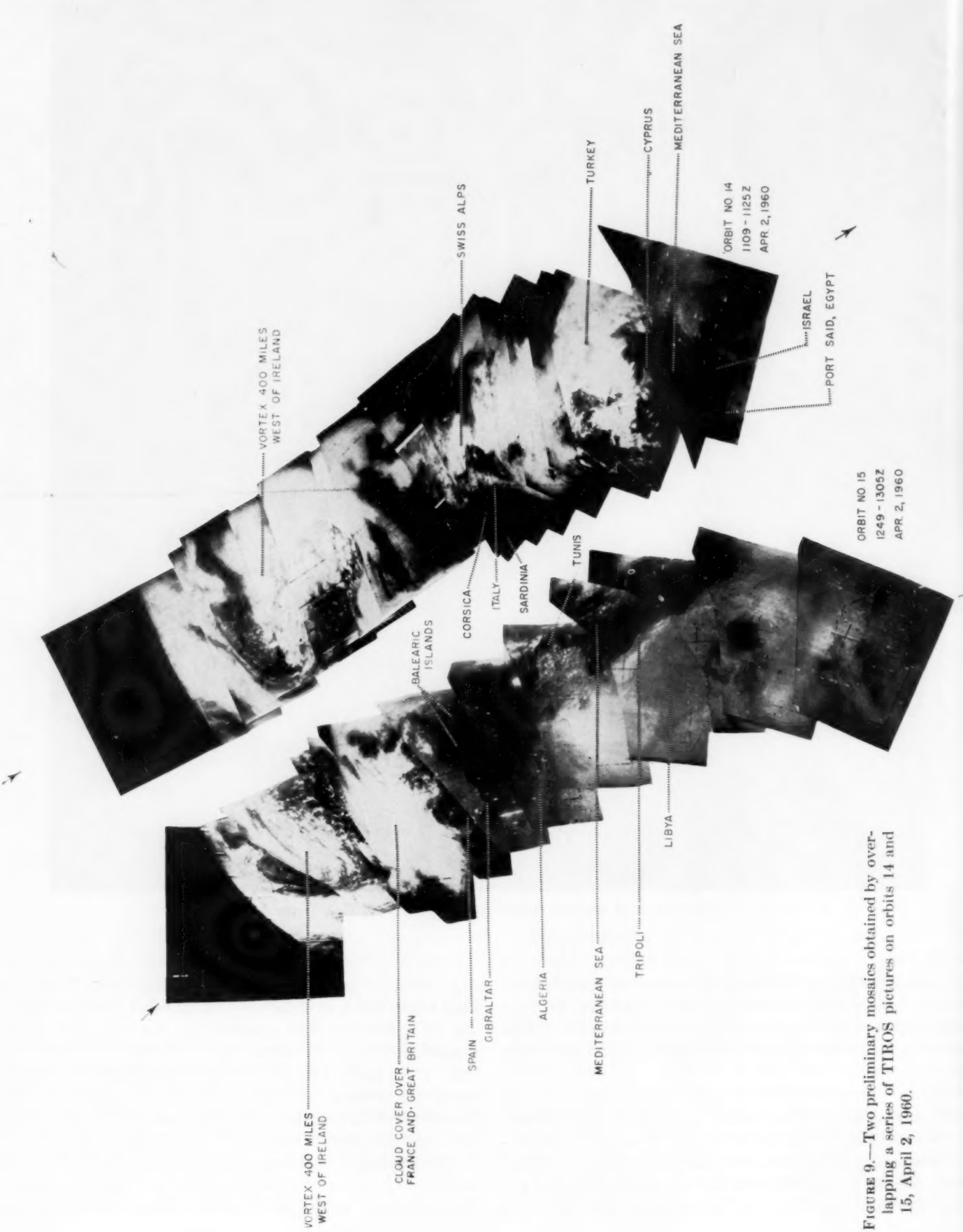

FIGURE 9.—Two preliminary mosaics obtained by overlapping a series of TIROS pictures on orbits 14 and 15, April 2, 1960.

FIGURE 10.—A preliminary schematic representation of cloud patterns revealed by TIROS pictures over an area extending from the west coast of the United States into the Atlantic Ocean (orbit 32) and from the mid-Atlantic to the Near East (orbit 28), April 3, 1960. The solid white lines outline the area covered by pictures on these two orbits. Examples of pictures used in preparing the schematic cloud map are shown along the borders of the area.

getting under way. In the months ahead pictures are expected to reveal much new information about many atmospheric processes—from fair weather situations to incipient storminess to the growth of fully mature storms and their final dissipation.

ACKNOWLEDGMENTS

Thanks are due to L. T. Tourville of the Meteorological Satellite Section who helped with preparation of the photographs for publication; W. H. Hoecker, Jr., of the Office of Meteorological Research who performed the meticulous and laborious work in preparing figure 10 from scores of individual photographs; Marshall Kathan, Chief of the Drafting Section, who supervised and personally assisted in the speedy preparation of illustrations from which the figures were extracted; L. E. Johnson, E. R. Orr, J. H. Morrison, and A. Y. Gardner of the Printing Section who gave excellent service in reproduction of the photographs; James E. Caskey, Jr., the editor, who not only suggested publication of the paper but together with Mrs. Bernice Baddy of his staff assisted greatly in its preparation.

REFERENCES

1. S. Fritz, "On Observing the Atmosphere from Satellites—I. Cloud Observations," *Weatherwise*, vol. 12, No. 4, August 1959, pp. 139–144, 163–165.
2. W. G. Stroud, "Initial Results of the TIROS I Meteorological Satellite," *Journal of Geophysical Research*, vol. 65, No. 5, May 1960, pp. 1643–1644.

548229—60——2

FORECASTING AIR POLLUTION POTENTIAL[1]

LAWRENCE E. NIEMEYER[2]

U.S. Weather Bureau Research Station, Robert A. Taft Sanitary Engineering Center, Public Health Center, Cincinnati, Ohio
[Manuscript received February 2, 1960]

ABSTRACT

A procedure for forecasting weather conditions conducive to high air pollution levels over a large area as a primary alerting system for potentially hazardous conditions is presented. Experiments conducted in the fall of 1957 and 1958 to test the procedure are described. The results indicate that forecasts of macroscale meteorological phenomena can be used to signify periods of high air pollution potential.

1. INTRODUCTION

Discharge of pollutants to the air during meteorological conditions conducive to their congestion could be reduced or eliminated for many sources of pollution provided adequate and dependable warning of the conditions were given. When conditions are favorable for rapid dispersion and diffusion of contaminants, higher rates of discharge are usually possible without creating undesirable effects. Occasionally meteorological conditions develop which inhibit dispersion of air-borne wastes for extended periods. Forecasts of the latter conditions, coupled with measurements of air quality, could provide a basis for pollution control.

A forecast of unfavorable atmospheric conditions would alert interested parties, both public and private, to take precautionary measures. Measurements of local air contaminants could then be initiated to monitor the air quality. If these measurements attained prescribed values and the forecast indicated that meteorological elements necessary to the accumulation of contaminants were expected to persist, then appropriate steps could be taken to reduce or eliminate the emission of pollutants until the measurements and the forecast show that normal activity could be resumed.

2. EFFECTS OF WEATHER ON DISPERSION OF AIR POLLUTANTS

Experience and investigation have shown that wind speed and atmospheric stability are the weather elements which may be considered as the primary meteorological factors that determine the dilution of air pollution in the lower atmosphere.

The volume of air into which contaminants are emitted is directly proportional to wind velocity, and the concentration of contaminants is generally inversely proportional to wind speed. If the wind speed doubles, other conditions being equal, the pollutants are emitted into twice the volume of air downstream from the source.

Stability depends on the temperature distribution with height. Normally temperature decreases with height approximately 3.3° F. per 1000 feet. When the decrease is greater than the dry adiabatic lapse rate (5.5° F. per 1000 feet), the air is unstable and vertical exchange and turbulence occur readily. When the decrease is less than 5.5° F. per 1000 feet or when the temperature increases with height, the air is stable and turbulence tends to be damped out. Theoretically the damping becomes greater as the temperature decrease with height lessens and is pronounced in an inversion layer. An inversion is that condition in the atmosphere when the temperature increases with height.

3. SELECTION OF FORECAST MODEL

Studies of air pollution episodes at Donora [1], Greater London [2], and other places have suggested that the simultaneous occurrence of very low wind speed, variable wind direction, pronounced stability, and fog is characteristic of these episodes. Furthermore, these conditions persisted for several days during each episode and were associated with quasi-stationary anticyclones.

On the basis of this knowledge a set of empirical criteria was selected as a foundation for forecasting air pollution potential. These criteria embody meteorological conditions which are associated with slowly moving anticyclones and are most likely to produce the conditions discussed above. These criteria are: (1) Surface winds less than 8 knots. (2) Winds at no level below the 500-mb. level greater than 25 knots. (3) Subsidence, the slow sinking or settling of air from aloft, below the 600-mb. level. (4) Simultaneous occurrence of the above with the forecast continuance of these conditions for 36 hours or more.

[1] Paper presented at Annual Meeting, American Industrial Hygiene Association, Chicago, Ill., April 30, 1959.

[2] Present affiliation: U.S. Weather Bureau Airport Station, San Francisco, Calif.

4. EXPERIMENTAL DESIGN

An experiment was designed to test the applicability of the given criteria as precursors of pollution episodes. The experiment was limited in time to the season during which stagnating anticyclones are most likely to occur [1, 3], and in area to the region in which stagnating anticyclones most frequently occur [3]. Secondary consideration was given to availability of air quality measurements.

The selected area (fig. 1) extends from 33° N. to 43° N. and from 78° W. to 88° W., or roughly, that area bounded by Myrtle Beach, S.C.; Tuscaloosa, Ala.; Milwaukee, Wis.; and Buffalo, N.Y.[3]

The operators in charge of National Air Sampling Network stations in this area volunteered to collect the air quality data necessary to determine the success or failure of forecasts for high pollution potential. Analytical work was done by the National Air Sampling Network (NASN) of Air Pollution Engineering Research at the Robert A. Taft Sanitary Engineering Center, Cincinnati, Ohio. Suspended particulate material collected over 24-hr. periods by high volume air samplers was used as the air quality measurement.

The daily weather was monitored over the selected region from October 1 to November 15, 1957 and from September 1 to November 15, 1958. Whenever weather conditions met the selected criteria in a minimum area (equivalent to a 4° square) and a forecast indicated that they would persist, a request for air quality measurements was relayed by telegram to appropriate NASN stations.

5. RESULTS

During the two test seasons, six periods were observed in which the criteria were met. Each period will be discussed in terms of the dominating weather influences, the air quality measurements obtained at each station during each episode, and comparable air quality measurements collected by the individual stations during the year. (National Air Sampling Network Stations take air quality measurements on a random basis; one 24-hr. sample is taken during each 2-week period.)

CASE 1

The first period occurred during October 11–15, 1957. An analysis of the weather data during this period shows that the region was under the influence of a slowly moving polar anticyclone, which began to affect the test area early on October 10. By the 11th, surface winds and winds aloft (table 1) were well within the criteria over northern Indiana and northern Ohio. By the 12th, light winds prevailed over southern Ohio and western Pennsylvania. Atmospheric soundings taken at Peoria (fig. 2), Dayton (fig. 3), and Pittsburgh (fig. 4) indicated the presence of subsidence. The surface anticyclone was

[3] Cities given in tables 2–5 and 7 outline the sub-areas within the test area where the criteria were met during a particular air pollution episode.

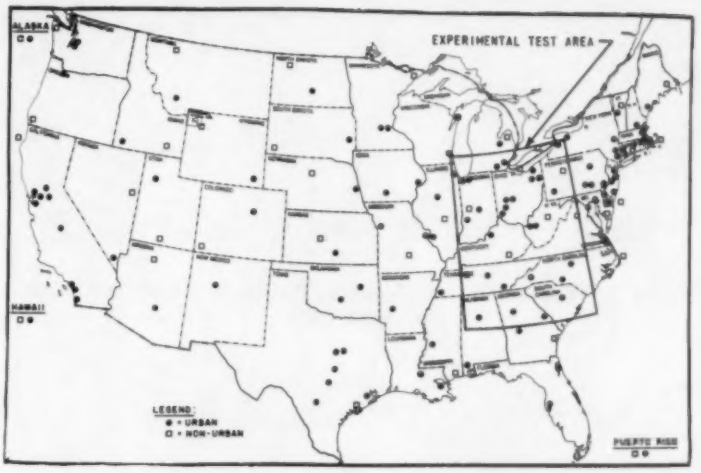

FIGURE 1.—National Air Sampling Network, June 1958. The experimental test area extends from 33° N. to 43° N. and from 78° W. to 88° W.

TABLE 1.—*Wind speed (knots) at selected stations 1300 EST, October 11–16, 1957*

Height (meters MSL)	Dayton, Ohio						Flint, Mich.						Pittsburgh, Pa.					
	11	12	13	14	15	16	11	12	13	14	15	16	11	12	13	14	15	16
6000	26	13	0	13	27	31	22	4	11	11	18	56	37	7	18	11	18	20
5000	20	13	7	11	25	40	26	7	18	16	25	45	29	13	16	11	18	25
4000	13	18	13	11	22	45	24	7	20	22	22	47	24	20	11	13	16	16
3000	11	11	9	9	22	47	22	7	22	16	31	51	18	11	9	9	4	20
2500	11	7	11	9	18	51	15	7	13	13	22	40	13	9	7	16	2	13
2000	11	11	11	7	20	49	11	7	4	13	18	31	13	7	2	11	4	11
1500	13	11	7	4	18	49	7	2	2	11	16	29	13	4	2	9	11	13
1000	9	13	7	2	13	45	11	4	4	11	18	42	13	7	4	7	9	13
500	15	13	7	7	7	22	9	4	4	7	11	27	13	7	7	4	2	9
*300	13	16	7	4	9	27	9	4	4	7	13	31	15	7	4	7	4	13
*150	15	13	7	7	7	20	9	4	4	7	11	22	13	7	7	4	2	9
SFC	15	9	9	7	9	16	7	1	7	9	11	11	13	7	7	7	0	9

*Height above surface.

TABLE 2.—*Particulate matter concentrations ($\mu g.m.^{-3}$) for National Air sampling stations, 1957*

Alerted October 11–15, 1957

Fort Wayne, Ind.	Indianapolis, Ind.	Columbus, Ohio	Lorain, Ohio	Lake County, Ind.		Pittsburgh, Pa.	Wheeling, W. Va.
				Site A	Site B		
70	87	77	55	66	**74	78	137
72	87	108	68	**121	101	79	143
79	106	114	69	128	107	82	150
85	111	125	75	142	147	103	152
89	119	132	78	205	152	103	155
91	123	132	84	215	155	104	157
102	123	136	105	230	162	126	159
105	125	145	114	255	180	136	163
109	127	159	116	272	192	159	165
110	128	164	117	*274	195	168	169
114	135	166	122	276	205	178	170
117	140	169	122	298	229	179	175
121	141	175	124	322	230	179	178
127	143	176	127	327	262	180	197
128	146	180	136	371	270	186	207
132	151	186	138	426	280	198	212
135	155	189	145	459	282	209	213
136	*158	191	159	479	298	252	215
138	166	211	162	978	*305	253	217
138	176	222	182		363	348	232
162	177	*226	215		545	397	277
*185	178	234	247			449	278
189	199	234	279			*534	*291
*198	200	241	298				292
202	217	*241	343				344
206	260	248	*398				
*244		248					
304		*274					
		310					

*Episode data.
**Post episode data. Samples taken after termination of alert.

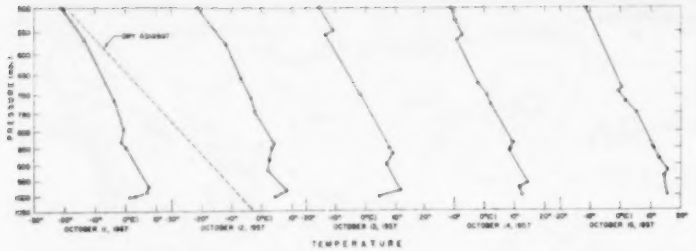

FIGURE 2.—Radiosonde observations, Peoria, Ill., 0700 EST, October 11–15, 1957.

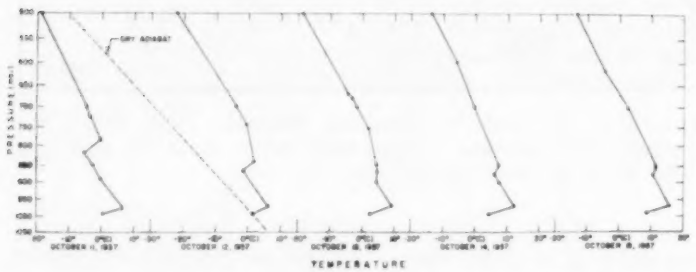

FIGURE 3.—Radiosonde observations, Dayton, Ohio, 0700 EST, October 11–15, 1957.

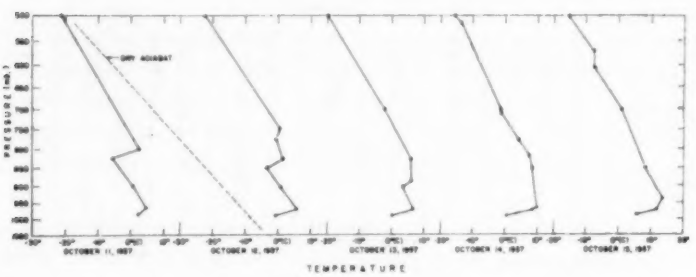

FIGURE 4.—Radiosonde observations, Pittsburgh, Pa., 0700 EST, October 11–15, 1957.

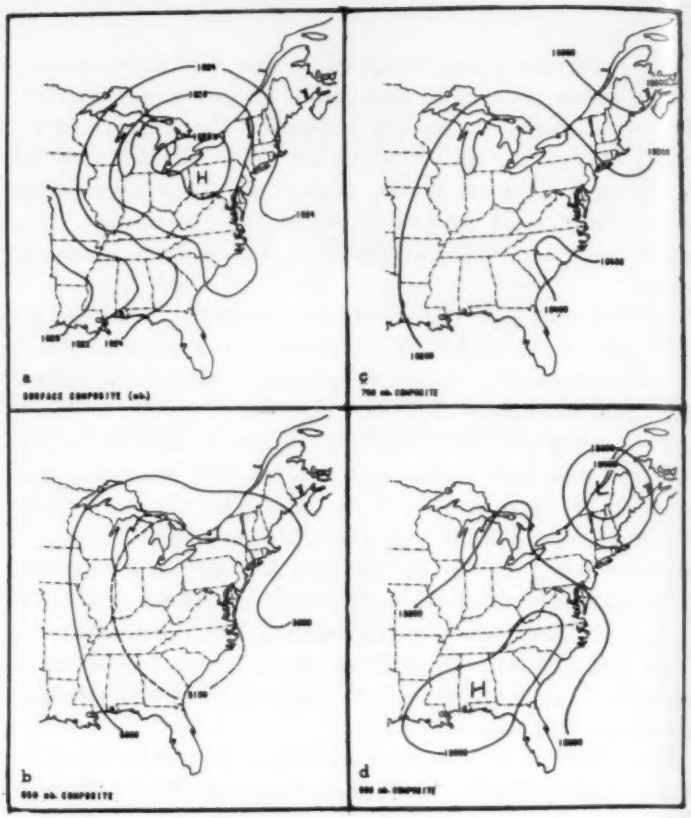

FIGURE 5.—Average meteorological charts, October 11–15, 1957. (a) Sea level composite pressure (mb.), 0100 EST. (b) 850-mb. composite height (ft.), 1900 EST. (c) 700-mb. composite height (ft.), 1900 EST. (d) 500-mb. composite height (ft.), 1900 EST.

accompanied by a well-developed ridge of high pressure aloft (fig. 5) and although the anticyclone did not stagnate, light winds, clear skies, and well-developed surface inversions prevailed during the period.

These meteorological conditions led to subnormal dispersion of contaminants and were instrumental in effecting high pollution levels. Table 2 presents the air quality data collected during the period in addition to data collected for the NASN by each station in 1957. In most instances, the requested measurements fell in the upper quartile for the year. For two stations, the values were the highest recorded in 1957.

An inspection of the local wind pattern in relation to the industrial and residential distribution in a Lake County, Indiana city gives a possible explanation for the difference in sampling values at the two stations during the October 13–14, 1957, sampling period. Wind directions ranged from ENE to SSE during this period. Winds from these directions favor the movement of industrial pollutants toward station B. The air passing over station A for these wind directions would pass primarily over a residential area before reaching the sampler.

The alert was terminated for the northwestern Indiana city and other cities on the afternoon of the 14th when it became apparent that the pressure gradient was intensifying and that strong surface winds would prevail over Indiana and western Ohio. Nevertheless a 24-hr. sample (October 14–15) was collected at two stations in a Lake County, Indiana city. The values recorded were 121 μg.m.$^{-3}$ at station A and 74 μg.m.$^{-3}$ at station B. These values are both within the lower decile of the 1957 data for these stations.

CASE 2

A request for air quality samples was issued in conjunction with a forecast on the afternoon of September 5, 1958. Since the telegrams did not reach the station operators before the close of the business day, no special samples were collected. A regular NASN sample collected at Greensboro, N.C., one of the stations to which a telegram was sent, fell in the upper decile of recorded 1958 data (see table 10).

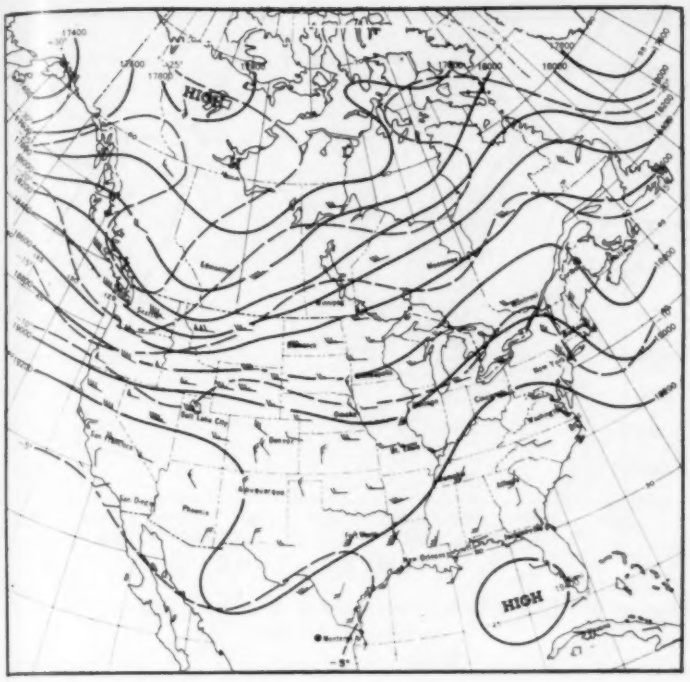

FIGURE 6.—500-mb. height chart, 1900 EST, September 19, 1958.

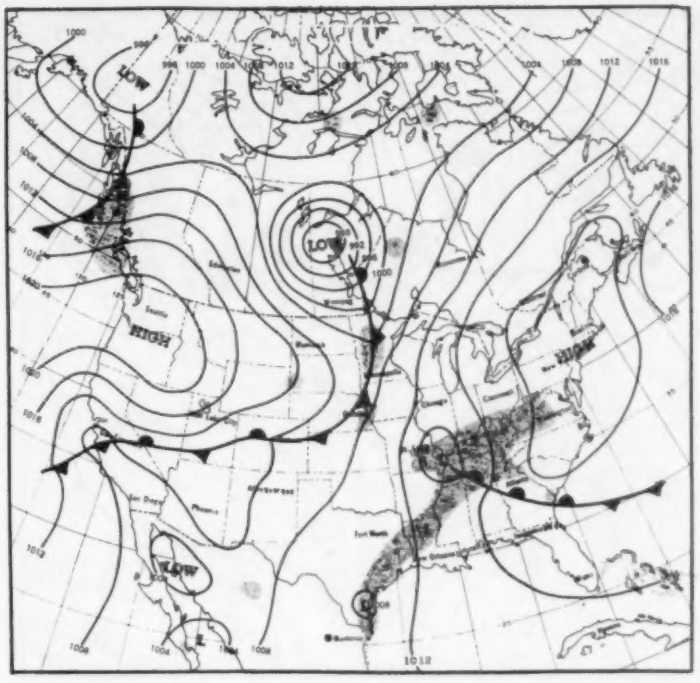

FIGURE 7.—Sea level pressure chart, 1300 EST, September 20, 1958.

CASE 3

On September 19, 1958, a surface high pressure system was centered over northern Ohio with an upper level ridge over the same general area. Available information indicated that the ridge would intensify and persist. However, cyclonic circulation developed at the 500-mb. level over the Texas Panhandle. It was detectable on the 1900 EST, September 19, 1958, 500-mb. chart and moved northeastward with the flow shown on figure 6. By the afternoon of September 20, a surface cyclone had developed and subsequently moved through the area of concern (fig. 7). Considerable precipitation, widespread cloudiness, and relatively strong wind flow were associated with the cyclone. The surface high pressure system moved rapidly eastward and was centered over Connecticut at 1300 EST, September 20 (fig. 7). A surface ridge extended over western Pennsylvania and eastern Ohio.

TABLE 3.—*Particulate matter concentrations ($\mu g.m.^{-3}$) for National Air Sampling Network Stations, 1958*

Alerted September 19–22, 1958

Akron, Ohio	Asheville, N.C.	Charleston, W. Va.	Charlotte, N.C.	Cincinnati, Ohio	Columbus, Ohio	Detroit, Mich.	Greensboro, N.C.	Jackson, Mich.	Pittsburgh, Pa.	Youngstown Ohio
44	*43	45	43	*42	*54	54	34	11	*83	79
*63	45	47	55	*81	78	65	*40	29	85	80
68	45	*52	*55	89	86	79	41	30	89	87
83	47	71	62	91	*100	80	41	32	89	89
84	48	71	66	93	108	91	*46	37	*97	*110
98	49	78	66	96	112	100	47	46	98	114
*99	*54	87	69	99	123	*100	63	46	102	*118
99	54	88	69	100	125	109	64	*53	103	119
100	64	89	82	113	126	114	67	55	115	120
101	66	92	86	117	*131	114	68	59	124	123
101	66	96	88	124	135	115	69	61	125	130
101	*71	*102	88	126	136	118	70	65	131	135
101	73	120	98	126	138	119	73	69	132	140
104	74	143	102	128	140	124	77	69	135	146
105	75	150	102	132	140	127	77	76	140	148
107	77	167	110	133	140	137	*77	76	140	150
113	78	178	113	134	146	140	80	77	144	153
126	82	195	127	135	148	143	89	77	150	154
127	95	*228	136	149	151	159	90	81	150	158
139	107	231	137	149	154	*186	97	84	152	159
140	108	232	*148	149	158	196	98	91	167	160
150	115	308	152	150	159	210	108	*92	178	166
164	121	336	168	180	174	217	126	93	212	170
*170	124	412	188	190	191	218	133	93	213	194
177	131	483	216	206	194	225	137	*93	230	212
198	179	708	236	259	219	246	156	94	257	*254
328	206		268	319	232			102	302	268
330	212		308		241			128	330	391
431					241				*343	
									344	

*Episode data.

Air quality data for the September 19–22, 1958 period are given in table 3 among the 1958 data collected by the participating stations. It can readily be seen that these samples are low with few exceptions. The relatively high values at Jackson, Youngstown, and Pittsburgh may be attributed to the fact that these stations are located well to the north and east of the area in which the cyclone developed. They were under the influence of the high pressure cell during the period September 19–20 when the high samples were collected. As the low pressure system moved eastward, surface wind speeds increased at these stations and the air quality improved.

CASE 4

The weather pattern of October 3, 1958 presented an opportunity to collect air quality data under conditions of only two of the criteria. Since there was visual evidence of air pollution, it was decided to request two 24-hr. air quality samples from each station listed in

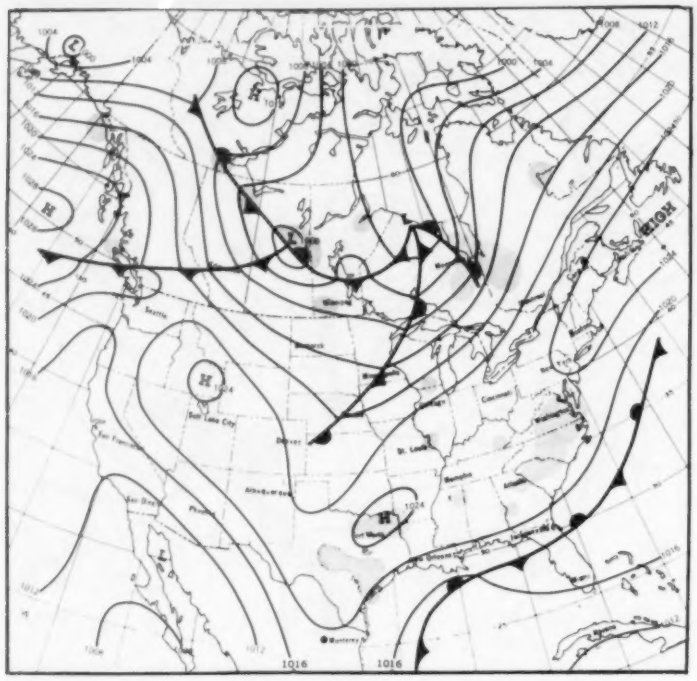

FIGURE 8.—Sea level pressure chart, 1300 EST, October 3, 1958.

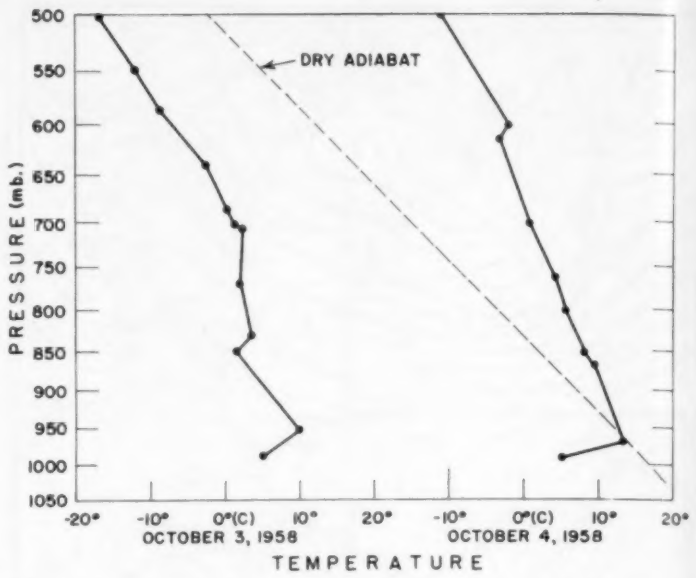

FIGURE 9.—Radiosonde observations, Dayton, Ohio, 0700 EST, October 3–4, 1958.

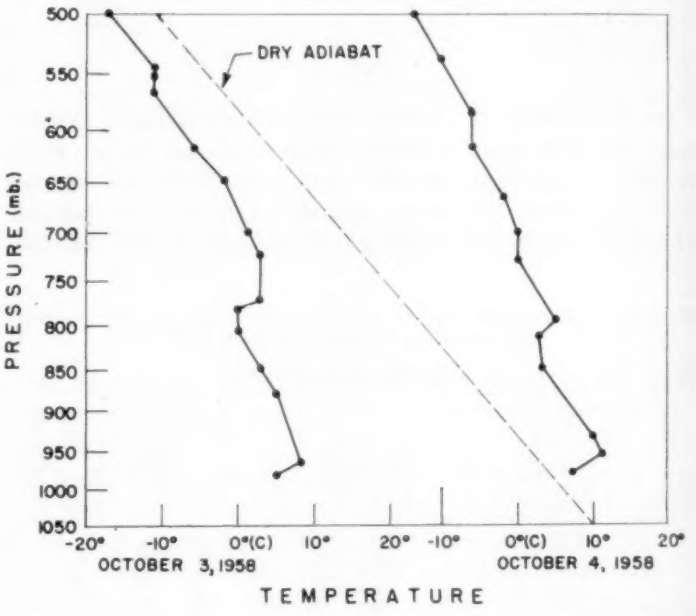

FIGURE 10.—Radiosonde observations, Pittsburgh, Pa., 0700 EST, October 3–4, 1958.

table 4 to determine the relative magnitude of the air quality under these conditions.

A surface high pressure cell was centered off the coast of Nova Scotia and a weak ridge of high pressure extended southwestward to Texas (fig. 8). Surface winds were light and variable and early morning radiosonde observations at Dayton (fig. 9) and Pittsburgh (fig. 10) indicated well developed surface inversions and subsidence inversions at 800–850 mb. Winds above 10,000 ft. exceeded 25 kt. and above 15,000 ft. exceeded 40 kt. Surface visibility was reduced by smoke and haze along the Ohio River from Louisville to Pittsburgh.

As was expected, the weather pattern did not persist. By the afternoon of the 4th, the surface pressure gradient along the Ohio River Valley had intensified and surface winds were at least 10 kt. (fig. 11).

Recorded values were not particularly high or low except for one high sample recorded at Cincinnati. In this instance the wind records indicate that pollutants were

TABLE 4.—*Particulate matter concentrations ($\mu g.m.^{-3}$) for National Air Sampling Network Stations, 1958*

Alerted October 3–5, 1958

Cincinnati, Ohio	Columbus, Ohio	Huntington, W. Va.	Pittsburgh, Pa.
89	78	50	85
91	86	58	89
93	108	*59	89
96	*108	61	98
99	112	63	102
100	123	67	103
*108	125	68	115
113	126	74	124
117	135	75	125
124	136	77	131
126	138	*90	132
126	140	91	135
128	140	91	140
132	140	102	140
133	146	102	144
134	148	103	150
135	151	104	150
149	154	117	152
149	158	126	167
149	159	126	178
150	*168	129	*198
180	174	139	*205
190	191	189	212
206	194	224	213
*252	219		230
259	232		257
319	241		302
	241		330
			344

*Episode data.

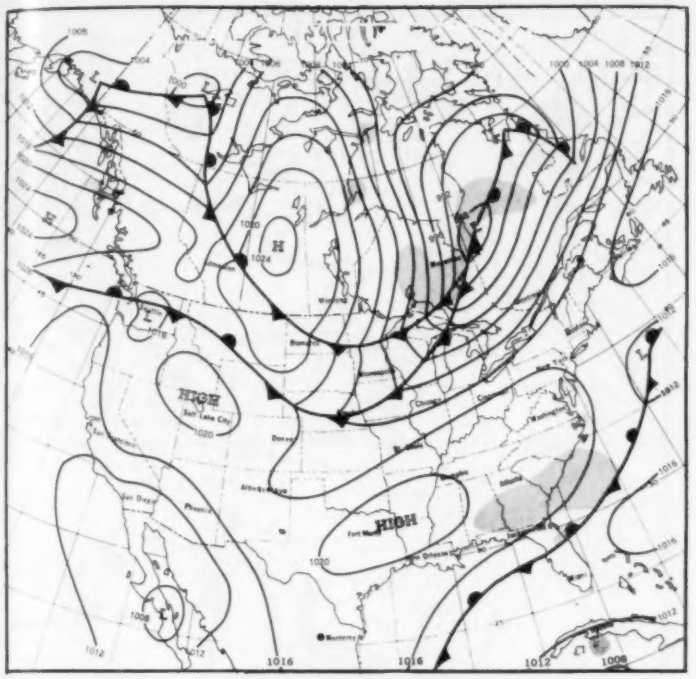

FIGURE 11.—Sea level pressure chart, 1300 EST, October 4, 1958.

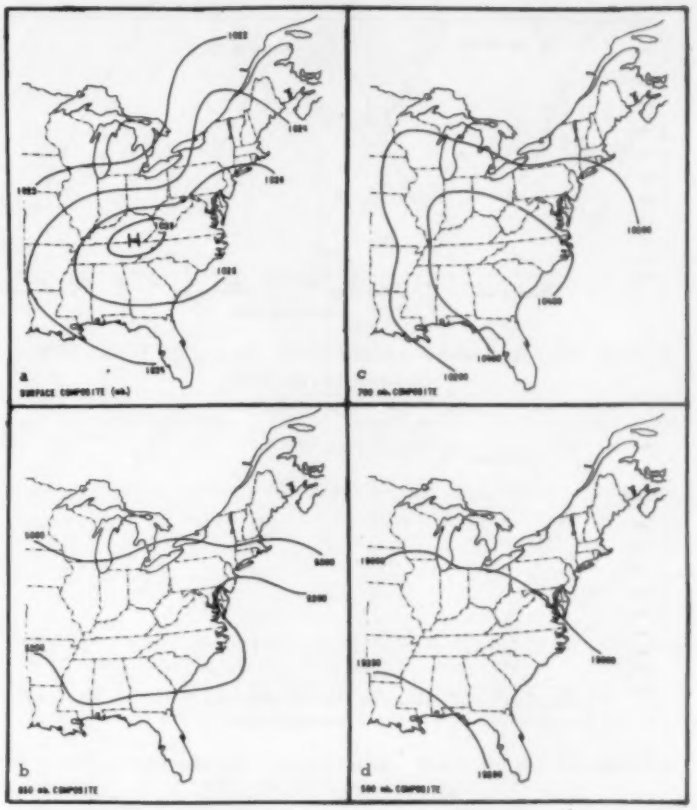

FIGURE 12.—Average meteorological charts, October 13–16, 1958. (a) Sea level composite pressure (mb.), 0100 EST. (b) 850-mb. composite height (ft.), 1900 EST. (c) 700-mb. composite height (ft), 1900 EST. (d) 500-mb. composite height (ft.), 1900 EST.

carried away from the city toward the west and southwest prior to the sampling period only to return over the city when winds shifted to the southwest. The extremely stable conditions did not permit the contaminants to mix to any appreciable height and therefore concentrations remained high.

CASE 5

In mid-October 1958, the weather over the southeastern United States was dominated by a high pressure cell, both at the surface and aloft, for a period of several days. The surface system entered the area from over the Great Plains. A strong ridge of high pressure aloft indicated that the area would be under the influence of high pressure for some time (fig. 12).

Analysis of weather charts in retrospect shows that the four stations given in table 5 were under the influence of the anticyclone from October 12 until October 17. However, winds aloft (table 6) less than 25 kt. did not become prevalent until the 13th. Subsidence was prevalent over

TABLE 5.—*Particulate matter concentrations ($\mu g.m.^{-3}$) for National Air Sampling Network Stations, 1958*

Alerted October 13-16, 1958

Asheville, N.C.	Chattanooga, Tenn.	Birmingham, Ala.	Atlanta, Ga.
45	90	46	35
45	98	53	55
47	101	68	67
48	114	96	75
49	158	*97	81
54	160	102	81
64	163	104	82
66	178	113	89
66	185	113	100
73	191	124	108
74	198	127	111
75	199	143	119
77	200	183	125
78	212	191	137
82	215	209	143
95	222	233	183
107	264	254	194
108	267	*319	200
115	268	342	210
121	376	369	241
124	*399	424	268
131	465	469	*367
179	509	640	
*188	*512		
206	528		
212	532		
*241	*549		

*Episode data.

TABLE 6.—*Wind speeds (knots) at selected stations, 0700 EST, October 13–16, 1958*

Height (meters msl)	Nashville, Tenn.				Birmingham, Ala.			Greensboro, N.C.			
	13	14	15	16	13	14	15	13	14	15	16
6000	18	18	13	16	22	M	M	36	20	16	11
5000	13	9	9	9	13	M	M	29	20	16	13
4000	13	11	2	13	11	7	M	29	18	9	9
3000	18	4	7	9	13	7	7	20	13	9	4
2500	18	2	4	11	11	4	7	18	9	4	9
2000	16	2	7	11	9	9	2	22	4	7	4
1500	11	4	4	11	13	11	7	16	2	7	9
1000	7	7	7	9	7	11	16	11	13	9	16
500	4	9	9	7	11	16	22	9	16	11	16
*300	4	9	9	7	11	16	22	11	18	13	20
*150	4	4	7	4	11	9	13	7	16	9	13
SFC	4	4	2	2	11	7	9	2	11	4	7

*Height above surface.
M = Missing.

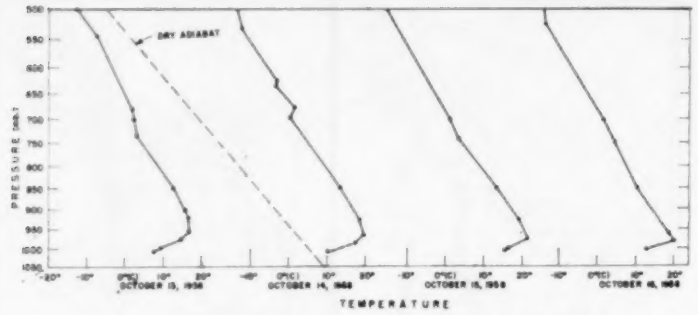

FIGURE 13.—Radiosonde observations, Nashville, Tenn., 0700 EST, October 13–16, 1958.

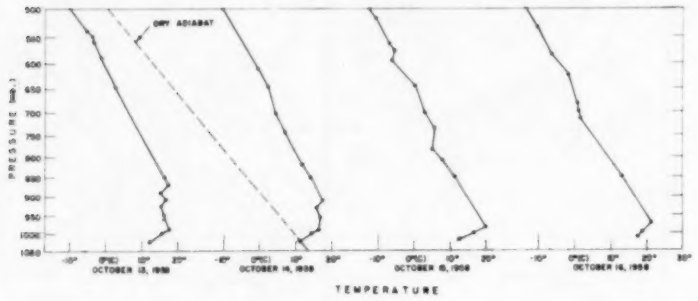

FIGURE 14.—Radiosonde observations, Montgomery, Ala., 0700 EST, October 13–16, 1958.

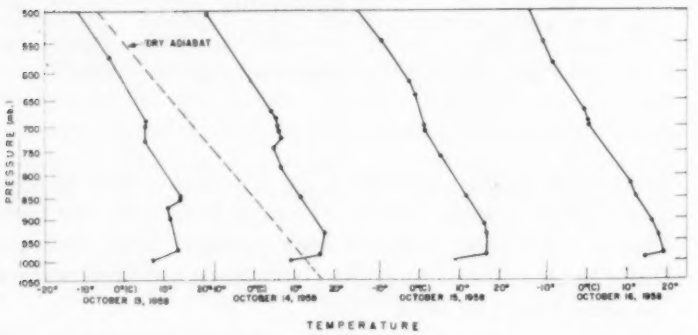

FIGURE 15.—Radiosonde observations, Athens, Ga., 0700 EST, October 13–16, 1958.

the general area until the 16th. Nocturnal surface inversions developed each night (figs. 13–15) but were apparently dissipated during the day. This circumstance was probably fortunate; otherwise, air pollution concentrations might have become severe in some areas. Fog was reported at Chattanooga and other stations but was dispelled early in the day.

In the period, October 13–16, conditions favoring maximum concentration of pollutants occurred during the night and early morning hours. Sufficient insolation was received to eliminate the surface inversions during the late morning and early afternoon. This permitted the pollutants to become dispersed into a deep layer. The winds, although light, were then instrumental in

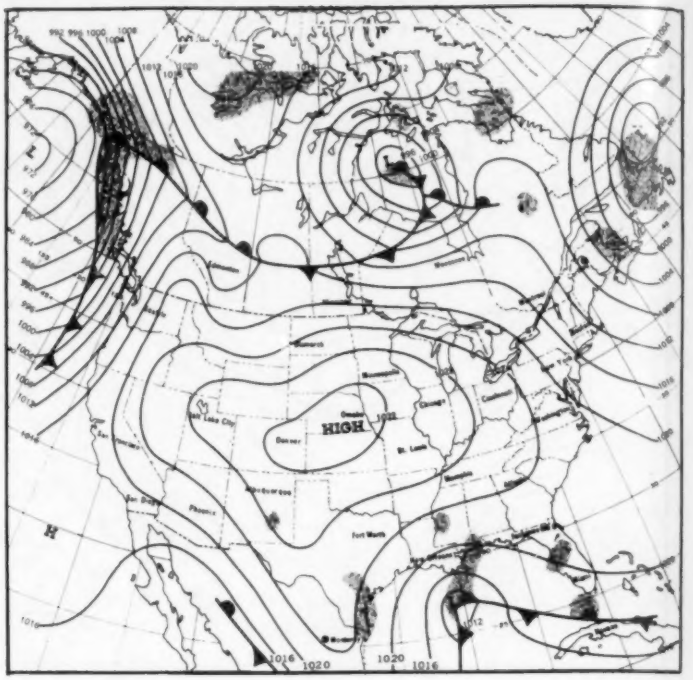

FIGURE 16.—Sea level pressure chart, 1300 EST, October 30, 1958.

carrying the contaminants away from the cities under study.

In this particular period the criteria were completely fulfilled. Success of the experiment for this period is shown by the high particulate loadings at the various stations (table 5). Loadings at Atlanta and Chattanooga were among the highest recorded data attained in two years.

The low sampling value at Birmingham may be attributed to the fact that the surface winds in the Birmingham area, while light, persisted from the east and southeast during the period in which the sample was collected. With these directions, the sampled air would have had a trajectory with minimum travel over the urban area.

CASE 6

The last experimental forecast for which air quality data were requested was issued on October 30, 1958. In this instance, a high pressure cell, centered in the central Great Plains, extended its influence eastward with a surface ridge of high pressure to the Atlantic Seaboard (fig. 16). Winds at the 5,000-ft., 10,000-ft., and intermediate levels were distributed into two main currents (fig. 17). One current was directed around a low pressure system located over Newfoundland; the other current flowed around the anticyclone centered over Nebraska. This diverging wind pattern was conducive to subsidence over the States of Ohio, Indiana, Kentucky, and West Virginia. Winds aloft charts and radiosonde observations for the period show that in this area winds ranged from 10 to 20 kt. be-

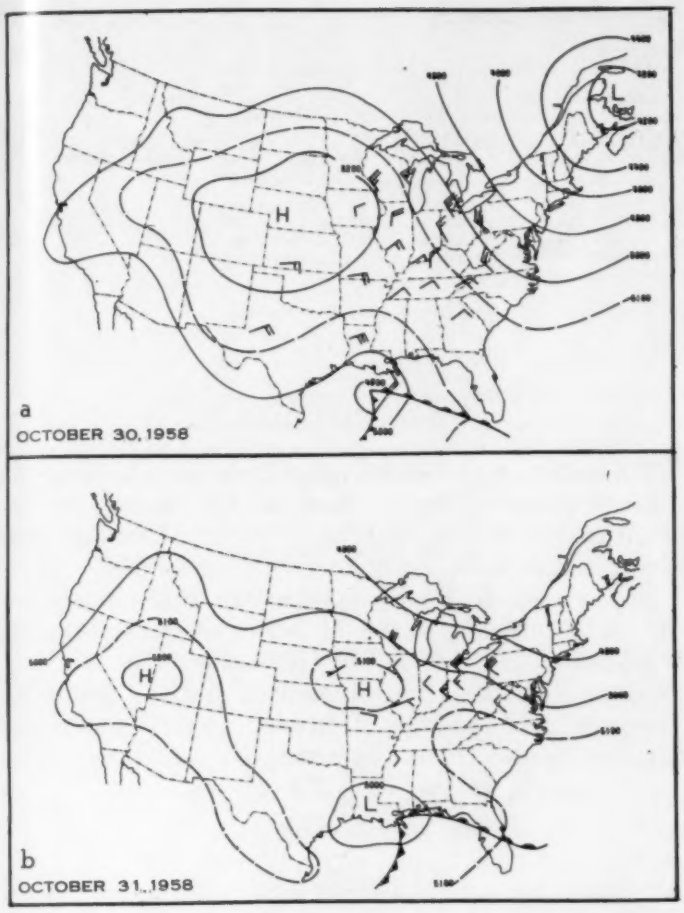

FIGURE 17.—850-mb. height chart, 0700 EST. (a) October 30, 1958. (b) October 31, 1958.

TABLE 7.—*Wind speeds (knots) at selected stations, 1300 EST, October 30–November 1, 1958*

Height (meters msl)	Indianapolis, Ind.		Cincinnati, Ohio			Dayton, Ohio		
	30	31	30	31	1	30	31	1
6000	11	20	16	27	M	18	25	22
5000	7	20	11	27	M	22	22	25
4000	13	13	13	16	M	20	16	16
3000	13	7	13	13	M	20	18	22
2500	16	11	16	16	M	18	20	29
2000	16	16	18	13	M	20	20	27
1500	20	22	16	13	20	22	20	29
1000	11	13	11	4	22	18	13	13
500	9	9	7	4	7	9	11	9
*300	9	9	7	7	9	11	11	9
*150	9	9	4	4	7	9	11	9
SFC	11	9	2	4	7	4	4	7

*Height above surface.
M = Missing

low the 5,000-ft. level (table 7), and well developed subsidence inversions and nocturnal surface inversions prevailed (fig. 18). These phenomena contributed materially to the retention of contaminants near the earth's surface. Table 8 presents the air quality data taken as a result of this alert. All values were recorded in the upper decile

548229—60——3

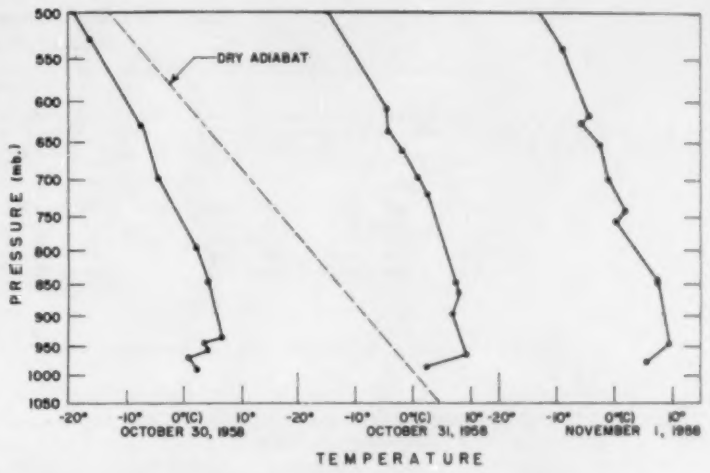

FIGURE 18.—Radiosonde observations, Dayton, Ohio, 0700 EST, October 30–November 1, 1958.

TABLE 8.—*Particulate matter concentrations ($\mu g.m.^{-3}$) for National Air Sampling Network Stations, 1958*

Alerted October 30–November 1, 1958

Charleston, W. Va.	Columbus, Ohio	Dayton, Ohio	Huntington, W. Va.	Indianapolis, Ind.	Louisville, Ky.	Cincinnati, Ohio
45	78	60	50	98	115	89
47	86	66	58	116	131	91
71	108	76	61	116	137	93
71	112	84	63	123	141	96
78	123	84	67	124	147	99
87	125	86	68	130	147	100
88	126	87	74	131	153	113
89	135	88	75	131	166	117
92	136	91	77	139	168	124
96	138	93	90	143	182	126
120	140	97	91	153	185	126
143	140	105	91	157	188	128
150	140	108	102	159	240	132
167	146	110	102	167	267	133
178	148	111	103	174	268	134
195	151	115	104	177	271	135
231	154	120	117	177	323	149
232	158	126	126	180	363	149
308	159	127	126	192	*378	149
336	*172	128	129	207	745	150
412	174	131	139	234		180
*420	191	148	154	250		190
483	194	150	*189	*297		206
*539	219	*199	224	332		259
708	232	*206		*354		*298
	241					*319
	241					
	*267					

*Episode Data.

for the year except for one value at Columbus; it was recorded in the upper quartile for the year.

6. CONCLUDING REMARKS

Examining the air quality data for the periods in which the weather was monitored, it is found that the highest loadings with few exceptions, occurred in those periods when the criteria were met (tables 9 and 10). Examination of source distribution and topography in the vicinity of the sampling sites together with a study of the wind direction patterns would probably reveal the explanation for the exceptions.

TABLE 9.—*Particulate matter concentrations* ($\mu g.m.^{-3}$)

October 1-November 15, 1957

Fort Wayne, Ind.		Indianapolis, Ind.		Lorain, Ohio		Columbus, Ohio		Lake County, Ind.				Pittsburgh, Pa.		Wheeling, W.Va.	
								Site A		Site B					
Date		Date		Date		Date		Date		Date		Date		Date	
10/5	110	11/12	106	10/30	105	10/19	176	10/15	**121	10/15	**74	11/9	82	11/3	165
11/14	121	10/21	125	11/7	136	10/12	*226	10/14	*274	11/5	230	10/28	136	10/1	232
10/12	*185	10/9	135	10/3	298	10/14	*241	11/5	426	10/1	298	10/12	*534	10/14	*291
10/13	*198	10/28	143	10/40	*398	11/10	248	10/1	459	10/14	*305				
10/14	*244	10/14	*158			10/13	*274								
						11/1	310								

*Episode data.
**Post episode—Samples taken after termination of alert.

TABLE 10.—*Particulate matter concentrations* ($\mu g.m.^{-3}$), *September 1–November 15, 1958*

Asheville, N.C.		Atlanta, Ga.		Birmingham, Ala.		Charleston, W. Va.		Chattanooga, Tenn.		Cincinnati, Ohio	
Date		Date		Date		Date		Date		Date	
9/21	54	10/22	111	10/16	*97	10/28	89	9/4	98	9/30	126
10/12	75	9/13	119	9/19	127	9/24	178	9/26	215	9/4	149
10/24	82	10/1	183	10/22	233	10/8	232	10/17	*399	9/3	150
10/7	95	10/15	*367	10/17	*319	10/31	*420	11/4	465	9/19	180
11/11	121			10/5	342	11/1	*539	10/16	*512	10/13	206
10/15	*188					11/14	708	10/20	528	10/30	*298
10/16	*241							11/10	532	10/31	*319
								10/14	*549		

Columbus, Ohio		Dayton, Ohio		Greensboro, N.C.		Huntington, W. Va.		Indianapolis, Ind.		Louisville, Ky.	
Date		Date		Date		Date		Date		Date	
9/1	78	10/29	76	10/5	64	10/5	90	9/12	130	10/24	147
10/13	146	10/25	84	10/9	70	10/11	117	9/26	159	9/23	188
9/15	151	9/20	86	10/31	97	11/2	154	9/9	180	11/7	267
10/31	*172	11/19	88	10/10	108	11/1	*189	10/17	192	10/31	*378
10/17	174	10/10	93	9/7	*133			11/6	250		
10/29	194	9/3	105					10/31	*297		
11/13	232	10/31	*199					11/1	*354		
11/1	*267	11/1	*206								

*Episode data.

This experiment was performed to demonstrate that forecasts of macroscale meteorological phenomena can be used to signify periods of high air pollution potential for a large area. Although derived from limited data, the results indicate that this can be done.

ACKNOWLEDGMENTS

The author expresses his appreciation to all those who assisted in collecting the data for this paper. Special credit goes to the operators of the National Air Sampling Network Stations who volunteered their services.

Appreciation is also expressed to Mr. J. Korshover and Mr. R. C. Wanta, Office of Meteorological Research, Washington, D.C.; Mr. T. W. Kleinsasser and Mr. R. J. Younkin, Weather Bureau Airport Station, Knoxville, Tennessee; and to Mr. E. S. Bennett and the staff of the Weather Bureau Office, Cincinnati, for their assistance in monitoring the weather in 1957 and 1958.

REFERENCES

1. H. H. Schrenk, H. Wexler, et al., "Air Pollution in Donora, Pennsylvania," *Public Health Bulletin* No. 306, Washington, D.C., 1949, 173 pp.
2. C. K. M. Douglas and K. H. Stewart, "London Fog of December 5–8, 1952," *Meteorological Magazine*, vol. 82, No. 969, March 1953, pp. 67–71.
3. J. Korshover, "Synoptic Climatology of Stagnating Anticyclones East of the Rocky Mountains in the United States for the Period 1936–56," U.S. Weather Bureau, Washington, D.C., Rev. November 1959, 26 pp. (printed manuscript).

REMARKS ON THE OPTIMUM SPACING OF UPPER-AIR OBSERVATIONS

D. C. HOUSE

Severe Local Storms Center, U.S. Weather Bureau, Kansas City, Mo.
[Manuscript received July 22, 1959; revised March 9, 1960]

ABSTRACT

The optimum time and space distribution of upper-air observations is considered in connection with the detection and prediction of instability lines—a mesoscale phenomenon. It is shown that the optimum spacing of observational stations is not only a function of the scale of the phenomena to be detected but of observational and analytical errors as well. When these errors are considered the optimum network spacing can be determined with regard to the dimensions of the atmospheric feature requiring detection. Because actual data are lacking, inferences concerning the maximum time and space distribution of upper-air sounding stations suitable for the detection of instability lines are drawn from a theoretical atmospheric model.

1. INTRODUCTION

The true dimensions of the instability line[1] have, for the most part, escaped detection except for its horizontal dimensions at the earth's surface [1] during the active stage. Some theoretical estimates of the dimensions of the instability line in the incipient stage can be inferred from [2]. However, the problem of detection of these lines by upper-air observations is also complicated by their relatively short life cycle. When one considers that the average dimensions of the instability line are of the order of 125 miles long, moving a distance of 175 miles in 5 hours, it can be seen that the chances of synoptically measuring the vertical distribution of horizontal gradients associated therewith are indeed small. The network spacing within the United States of 220 nautical miles (average) and time spacing of 12 hours provide a very low probability of the detection of the atmospheric processes involved in the production, propagation, and dissipation of such phenomena. On the other hand, the time and space distribution of surface weather reporting stations provides a much better probability of the detection and the prediction of the line. Unfortunately, without a knowledge of the vertical extent and relative strength of the dynamic processes involved in the production of intense vertical motion, the forecaster stands little chance of gaging correctly the intensity of activity associated with the thunderstorms. Likewise, the prediction of the formation and dissipation of this activity is handicapped.

Since the prediction of such phenomena is of economic importance, and the successful prediction is dependent upon initial observations of the meteorological processes involved, the purpose of this paper is to discuss the upper-air observational network needed to improve the detection and prediction of these phenomena.

[1] The instability line has been designated by the World Meteorological Organization as a line of incipient, active, or dissipating nonfrontal instability conditions. It is primarily an analytical tool for indicating the incipient and dissipating stages of squall line phenomena.

2. OPTIMUM NETWORK SPACING

The map analysis of any quantity derived from synoptic weather observations is subject to two principal errors. One error is the error of measurement inherent in the observations themselves, and the other is the truncation error due to smoothing of the isolines of the observed values. The design of an observational network must take both of these errors into account. The optimum space and time distribution of observations is dependent upon the relation between the errors of observation and the gradient of the quantity being analyzed. If the gradients involved in the system being analyzed are smaller than the gradient of errors, the analysis becomes one of errors rather than of the system itself.

The optimum spatial distribution of radiosonde stations is that distance between adjacent stations which minimizes the variance about the true horizontal gradient of the analyzed gradient (true gradient plus gradient of errors). Consider a situation in which two observation stations a distance d apart lie along the x-axis, one at $x=d/2$ and the other at $x=-d/2$. One error arises from observational errors and the other from truncation errors. Let E_1 be the root mean square of the observational errors and E_2 be the root mean square of the truncation errors that arise in computing the first derivative at the midpoint between stations of a quantity y from the observations at the two stations. The total error will then be

$$E_3=\sqrt{E_1^2+E_2^2}. \tag{1}$$

Let the root mean square error of observation of y be σ, then

$$E_1=\frac{\sqrt{2}\sigma}{d}. \tag{2}$$

The truncation error is found by forming Taylor's series involving y at $d/2$ and $-d/2$. Subtracting the second from the first series (after dropping terms of higher order than the third) and dividing by d gives a finite difference representation of the gradient that differs from $\partial y/\partial x$ by a third order term, the truncation error. The root mean square of the truncation error is found to be

$$E_2=\frac{d^2}{4!}\sqrt{\frac{1}{n}\sum_{i=1}^{n}\left(\frac{\partial^3 y}{\partial x^3}\right)_i^2}=\frac{d^2}{4!}\left|\frac{\partial^3 y}{\partial x^3}\right|. \tag{3}$$

The total error is then

$$E=\sqrt{E_1^2+E_2^2}=\left(\frac{2\sigma^2}{d^2}+\frac{d^4(y''')^2}{(4!)^2}\right)^{1/2} \tag{4}$$

where $y'''\equiv\partial^3 y/\partial x^3$.

Since it is desired that d be chosen such that E^2 is minimized, the first derivative of the root mean square of the total error will be made zero.
Thus

$$\frac{dE}{dd}=0=-\frac{4\sigma^2}{d^3}+4d^3\left(\frac{y'''}{4!}\right)^2 \tag{5}$$

Solving for d gives the condition for optimum d,

$$d=2\left(\frac{3\sigma}{|y'''|}\right)^{1/3} \tag{6}$$

Upon substitution of the finite difference form of the third derivative for y''', equation (6) is identical to that contained in [3]. Under certain conditions a solution can be found by using the equation in the manner suggested in [3], i.e., as a first guess, the measuring interval is set to d and the values of the quantity are selected from the observational record. From this an approximate third derivative is computed and with σ given, a new d is found. The process is repeated until the successively derived values of d converge. However, for the very short waves of interest here, the values diverge; moreover, for short measuring intervals the evaluation of the third derivative by use of the approximate difference form becomes difficult to achieve with accuracy. Under such conditions it is necessary to utilize a more rigorous procedure for determination of the third derivative in seeking a solution to equation (6).

Given knowledge of the variation in time or space of any continuous function it is possible to approximate the time or space variation mathematically. The mathematical expression that describes the variation can then be differentiated three times to obtain the third derivative, the value of which can then be determined precisely for any point along the curve. This value can then be substituted into equation (6) and with σ given, d is found. This is then the d required within the limits of observational error to give the optimum finite difference representation of the gradient of a quantity y having a complexity described by the third derivative around the point of application. A greater spacing of stations would result in an analysis such that the real feature would be lost through smoothing of the isopleths. Any spacing less than the optimum would tend to become an analysis of observational errors. An inspection of equation (6) reveals that it has no practical application when y''' is zero or infinite since the optimum spacing would then be infinite or zero, respectively.

3. COMPUTATION OF NETWORK SPACING

As indicated above a knowledge of not only the dimensions of the atmospheric features but a knowledge of observational errors is required to determine the optimum observational network. Unfortunately, there is little published information concerning the standard error of upper-air observations. Data secured as a result of radiosonde compatibility tests [4] indicate that an error of ± 50 feet at the 500-mb. level is reasonable. A later study [5] using an indirect method estimated this error to be about 15 meters or approximately 49 feet. A value of 50 feet will be used subsequently for σ in evaluating equation (6).

The detection and prediction of instability lines are dependent, in the main, upon a knowledge of the time change of the existing thermal instability. The prediction of the intensities of weather phenomena associated with these lines is also dependent upon the time rate of change of the vertical thermal instability. Consequently, it appears desirable to specify the upper-air properties of the instability line in terms of a parameter that involves the horizontal as well as the vertical thermal structure. Since thickness permits us to interpret the horizontal and vertical temperature structure it can be utilized. The significance of thickness with respect to cyclonic development is discussed in [6], and its relation to instability line formation is indicated in [2]. Little is known about the true dimensions of thickness and thickness gradients with respect to the instability line; however, theoretical computations [2] can provide the basis for a beginning.

Data from figure 7 of [2], reproduced here as figure 1, were used to develop table 1, a tabulation of the thickness computed for the layer 1,000–500 mb. for points 6, 7, 8, 9, and 10 of that study, located a distance of 60 n. mi. apart. These data were utilized to construct the vertical section shown in figure 2. It was found that this curve is approximated closely by the equation

TABLE 1.—*Thickness values for layer 1,000–500 mb. through a space section normal to an instability line computed from the theoretical data of figure 1. Points 6, 7, 8, 9, and 10 are located 60 n. mi. apart.*

Location	6	7	8	9	10
Thickness	18,670	18,705	18,615	18,625	18,631

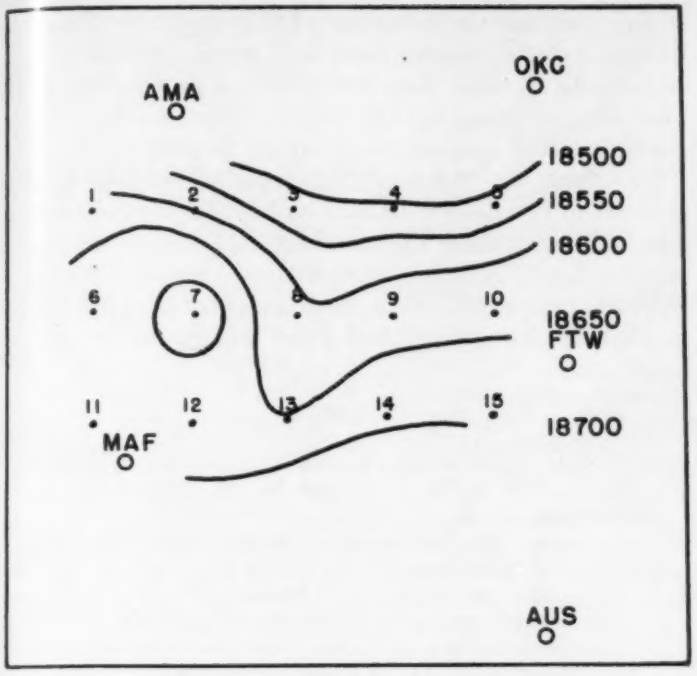

FIGURE 1.—Thickness field associated with a theoretically computed instability line. Computations were made at numbered grid points which are 60 n. mi. apart. (After [2].)

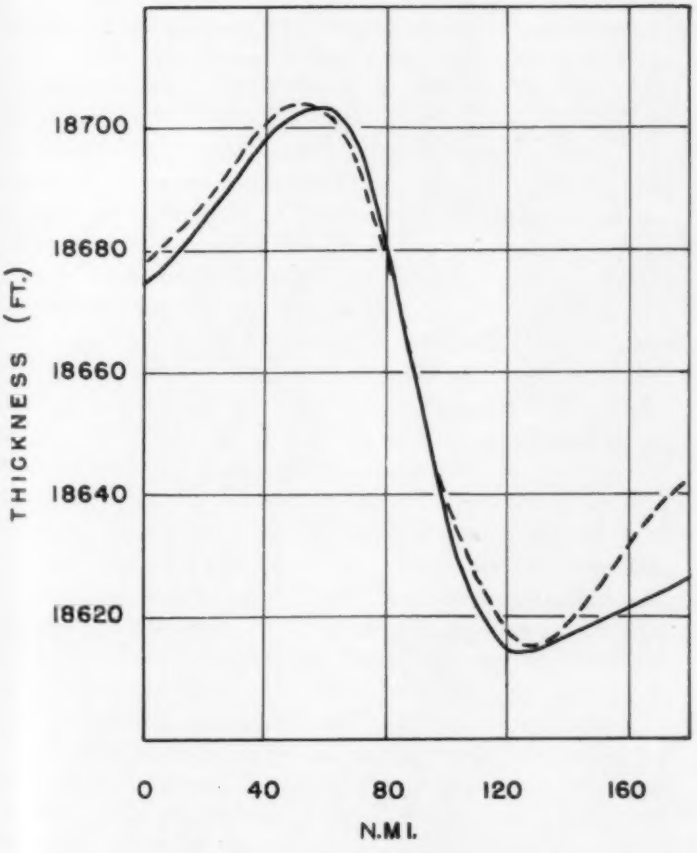

FIGURE 2.—Solid curve is vertical profile of thickness along sections 6–10 of figure 1. Dashed curve is plot of equation (7) given in the text.

$$y=y_0-A_1\cos\left(\frac{2\pi}{L_1}x\right)+A_2\cos\left(\frac{2\pi}{L_2}x\right) \quad (7)$$

where $y_0=18{,}660$ feet, $A_1=22.5$ feet, $L_1=120$ n. mi., $A_2=40$ feet, and $L_2=360$ n. mi. Differentiation of equation (7) three times gives

$$y'''=-A_1\left(\frac{2\pi}{L_1}\right)^3\sin\left(\frac{2\pi}{L_1}x\right)+A_2\left(\frac{2\pi}{L_2}\right)^3\sin\left(\frac{2\pi}{L_2}x\right). \quad (8)$$

y''' was evaluated from equation (8) at $x=90$ n. mi. (location of inflection point) and $x=130$ n. mi. (trough location) and its average value was computed for the interval $x=50$ to $x=130$ n. mi. Substitution of these values of y''' into equation (6) gave the optimum spacing of stations. The results are given in table 2.

It can be seen from equations (6) and (8) and table 2 that the optimum spacing of stations varies according to the choice of location at which the third derivative is computed. For this reason it appears that the spacing computed for the average value y''' average for the portion of the curve most significant to the analysis problem at hand should be considered the optimum. In the case at hand a spacing of stations 93 miles apart would assure the detection of the feature when both observational and analytical errors are considered. The corresponding optimum time interval for observations, on the assumption of a translation of the pattern at a speed of 30 m.p.h., is 3.1 hours.

At this writing knowledge of the dimensions of incipient instability lines is so meager there is no way of knowing the deviation of the above data from that averaged from a large number of cases. It is clearly evident, however, that establishment of such an average or mean dimension is dependent on a greater time and space density of stations.

Preliminary analyses of data secured from a few aircraft traverses through instability lines during the incipient stage indicate that important waves may exist whose ratio of wave length to amplitude is smaller than that used in the theoretical computation above. The significance of the theoretical study is that operational experience indicates that a feature of that size or larger is probably in existence in about one-half the cases a short time before the development of thunderstorms along the instability line.

TABLE 2.—*The optimum spacing (d) of stations corresponding to values of $|y'''|$ at the inflection point ($x=90$ n. mi.) and trough point ($x=130$ n. mi.), and its average over the interval $x=50$, 130 n. mi.*

	x n. mi.	$\lvert y'''\rvert$ ft. (n. mi.)$^{-3}$	d n. mi.
Inflection point	90	3.44×10^{-3}	70.4
Trough point	130	1.45×10^{-3}	93.8
Average	50–130	1.53×10^{-3}	92.2

4. CONCLUSIONS

The above considerations indicate clearly that the optimum time and space density of observations is a function not only of the observational errors but a function of the truncation error as well. Obviously, then, the time and space density of upper-air observations and analyses thereof must be such as to insure the capability of detecting the smallest atmospheric feature important to the particular forecast problem. When these errors are considered the optimum network spacing then can be determined with regard to the dimensions of the atmospheric features requiring detection.

From a research or forecasting standpoint, it is obvious that a greater density of upper-air sounding stations is a necessity if we are to determine with certainty the dynamic processes that result in the formation, propagation, and dissipation of the instability line. Although a network as dense as that suggested here by the computation of optimum spacing for incipient instability lines may never become economically feasible for routine forecasting, it is also obvious that the existing network is much too sparse to provide the basis for any appreciable improvement in the forecast. This is because the extent to which the forecaster is able to decrease his forecast errors is limited by the extent to which the observational network approaches an optimum design with respect to the scale of the phenomena which he must predict.

A recent study by Gleeson [7] suggests a method for computing the probabilities of observing an atmospheric feature of a given size. Using this approach and the dimensions of the theoretically derived instability line [2], it appears that the detection of the existence of such a feature by the existing time and space distribution of radiosonde stations does not exceed a probability of 10 percent. Doubling the number of stations would increase the probability of detection by about 20 percent.

The foregoing considerations indicate clearly that a network of rawinsonde stations at least double the existing number, and taking observations at 6-hourly intervals, supplemented by winds aloft stations, would result in a significant improvement in the detection of the phenomena in the incipient stage, and thus the prediction of the active stage.

REFERENCES

1. M. Tepper, "Pressure Jump Lines in Midwestern United States," Weather Bureau *Research Paper* No. 37, Washington, D.C., June 1954, 70 pp.
2. D.C. House, "The Mechanics of Instability-Line Formation," *Journal of Meteorology*, vol. 16, No. 2, April 1959, pp. 108–120.
3. C. L. Godske, T. Bergeron, J. Bjerknes, R. C. Bundgaard, *Dynamic Meteorology and Weather Forecasting*, American Meteorological Society, Boston, Mass., and Carnegie Institution, Washington, D.C. 1957, 800 pp. (p. 626).
4. Air Coordinating Committee, Subcommittee on Aviation Meteorology, *Radiosonde Compatibility Tests Made at Oklahoma City, Oklahoma, June 4–20, 1951*, U.S. Weather Bureau, Washington, D.C., March 1952, 273 pp.
5. L. Holloway, "An Indirect Method for Determining Radiosonde Error and Optimum Station Spacing," U.S. Weather Bureau, Washington, D.C., January 1957, 9 pp. (printed manuscript).
6. S. Petterssen, *Weather Analysis and Forecasting*, 2d Ed. Vol 1, McGraw-Hill, New York, 1956, 428 pp. (Chap. 16).
7. T. A. Gleeson, "Observational Probabilities and Uncertainty Relations for Meteorology," *Journal of Meteorology*, vol. 16, No. 2, April 1959, pp. 149–154.

COMPARISON OF EVAPORATION FROM WEATHER BUREAU CLASS A AND BUREAU OF PLANT INDUSTRY (BPI) SUNKEN PANS, FORT ASSINNIBOINE, MONTANA

R. A. DIGHTMAN

Weather Bureau Airport Station, Helena, Mont.

[Manuscript received October 19, 1959; revised February 15, 1960]

ABSTRACT

Comparative evaporation measurements for both BPI sunken and WB Class A pans at Fort Assiniboine, Mont., for an 8-year period, are reported and are subjected to several elementary analyses which indicate that pan-to-pan ratios determined in one area are not necessarily applicable to any other. The latter point is shown by a comparison of ratios from several widely separated points in the nation. Comparative pan temperatures (maximum, minimum, and mean) are also tabulated and discussed.

1. INTRODUCTION

The need for more useful water loss information has been reflected during the last 20 years in a fairly large number of studies devoted to evaporation and transpiration. In an effort to determine the relationship between Weather Bureau (WB) Class A and Bureau of Plant Industry (BPI) sunken evaporation pans at one of the more northerly latitudes of the United States, evaporation measurements were made from both types of pans, exposed adjacent to each other in the instrument enclosure of the climatological station at North Montana Branch Experiment Station, Fort Assinniboine, Mont. (near Havre).

As both types of pans have been used extensively across the nation, the physical characteristics of each require only brief description. Both are illustrated very well by Kohler [1] in his photographs of pan installations at Lake Hefner. Briefly, the WB Class A pan is 48 inches in diameter and 10 inches deep. This pan is exposed on spaced 2 in. x 4 in. lumber so that its bottom is a little above the ground and air can circulate beneath the pan. The water is maintained at a depth of about 7 or 8 inches. On the other hand, the BPI pan is 72 inches in diameter and is 24 inches deep. It is set in the ground to a depth of 20 inches, leaving about 4 inches of the pan rim standing above the soil surface. The BPI water level is maintained ideally at near the ground level. Micrometers exposed in stilling wells were used for measuring daily evaporation amounts in both pans. Both were exposed in a fenced enclosure, with a free flow of air over both water surfaces. When the BPI pan developed a leak early in the 1957 season, it was abandoned, and the Class A pan has since been used for evaporation measurements for the Experiment Station.

Figure 1 is a photograph of the Fort Assinniboine instrument enclosure as it was throughout the period of comparisons. The installation is standard except that in an attempt to have one anemometer serve both pans, this instrument was not mounted on the Class A pan base, was some 15 inches higher than standard above the pan rim, and was located several feet from both pans. While these factors would tend to produce slightly higher wind movements than a standard installation would have, the fact

FIGURE 1.—Fort Assinniboine, Mont. Instrument exposure (looking north). BPI pan is in center foreground of enclosure, Class A pan on left, and ground level anemometer behind the Class A pan.

remains that, in cases of this kind where wind movement is fairly large in any case, effects of this factor on total evaporation are small.

Considering the large number of evaporation installations of either Class A or BPI sunken types, it is quickly recognized that available evaporation data in terms of either pan can be increased considerably across the nation if simple conversion factors for computing reasonable values of one pan from observations of the other can be determined either experimentally or theoretically. In fact, if the required theoretical parameters can be more easily measured or estimated than actual evaporation, for some locations it may be possible to achieve reasonable and usable estimates without the need for several years of actual measurements. The purposes of this paper are to report actual comparisons at Fort Assinniboine over an 8-year period; to compute theoretical evaporation for the part of the period for which the necessary parameters are available; to compare these theoretical, or analytical, results with actual measurements for the same period; to summarize water temperatures for both pans for about five years; and to discuss the results and some of their possible applications.

2. COMPARATIVE EVAPORATION MEASUREMENTS

Table 1 lists monthly evaporation totals for both pans for the 8-year period, 1949–56. Measurements are not practical for the period October–March, inclusive, because of ice problems associated with freezing temperatures, and only occasionally is a partial month of measurements obtainable in April. Comparison of actual measurements is available, therefore, only for the five months, May–September. In a few cases adjustments were made for inconsistent data, by deleting measurements from both pans. This expedient was employed for only four dates for the entire period, and does not affect comparison because daily data from both pans were deleted when the measurement from either was questionable.

TABLE 1.—*Monthly evaporation (in.) Fort Assinniboine, Mont., latitude 48°30′ N., longitude 109°48′ W., elevation 2687 ft. M.S.L.*

Year	April	May	June	July	August	September	Seasonal
BPI Sunken Pan (x)							
1949	6.40	6.90	8.13	9.31	9.44	6.17	
1950	3.88	5.82	5.63	7.03	6.03	4.56	
1951		6.26	4.55	7.50	6.62	3.36	
1952	5.43	5.87	7.84	8.08	7.66	5.17	
1953	2.15	4.39	5.33	7.71	7.74	5.23	
1954		5.97	5.30	8.39	5.59	3.99	
1955		4.53	6.68	5.79	8.04	5.06	
1956		4.56	7.95	7.71	7.98	4.35	
Average		5.55	6.43	7.69	7.39	4.74	31.80
Class A Pan (y)							
1949	9.53	10.00	11.24	12.95	13.01	8.25	
1950	5.95	8.94	8.73	9.86	8.47	6.28	
1951		9.93	6.77	11.36	9.27	4.78	
1952	7.41	8.53	11.56	12.04	10.95	7.50	
1953	3.42	6.82	7.88	11.46	11.60	7.68	
1954		8.66	7.67	12.82	8.51	5.83	
1955		6.34	9.15	8.64	11.94	6.78	
1956		7.43	12.13	11.46	10.71	6.75	
Average		8.33	9.39	11.32	10.56	6.73	46.33
y/x		1.50	1.46	1.47	1.43	1.42	1.46
x/y		.666	.684	.679	.700	.704	.686

TABLE 2.—*Average inches of evaporation, 1949–1956, and y/x ratios*

	Montana		y/x	
	BPI (x)	Class A (y)	Montana, 8 yrs.	Kansas, 14 yrs.
May	5.55	8.33	1.50	1.48
June	6.43	9.39	1.46	1.46
July	7.69	11.32	1.47	1.45
August	7.39	10.56	1.43	1.44
September	4.74	6.73	1.42	1.45
Season	31.80	46.33	1.46	1.46

TABLE 3.—*Evaporation ratios, other experiments (after [1])*

y/x	Location	Period
1.30	Lake Kickapoo, Tex.	January 1950–December 1951.
1.20	Buchanan Dam, Tex.	January–December 1950.
1.33	Denver, Colo.	June–October 1916.
1.25	Balmorhea, Tex.	April 1941–December 1948.
1.28	Pardee Reservoir, Calif.	January 1930–December 1944.
1.29	Yuma Field Station, Calif.	January 1937–December 1939.
1.21	Fullerton, Calif.	January 1937–December 1939.
1.35	Lake Hefner, Okla.	May 1950–August 1951.

With y designating Class A evaporation and x BPI evaporation, monthly y/x ratios varied between 1.42 (September) and 1.50 (May), following closely the ratios reported in the preliminary report of the first 4 years of comparisons [2]. The seasonal y/x ratio, 1.46, agreed exactly with the results of 14 years of similar comparisons at Hays, Kans., for the slightly longer April–September 6-month period (the 5-month y/x ratio at Hays is 1.45) [3]. It seems, therefore, that the seasonal y/x relationship has been determined experimentally, at least for areas similar to Hays and Fort Assinniboine, within narrow limits (see table 2). However, in comparing these two seasonal results with results at several other locations (table 3), we find important differences, with the y/x ratio ranging from 1.20 at Buchanan Dam, Tex., to 1.35 at Lake Hefner, Okla. Noting that seasons for all eight points listed by Kohler [1] varied from one to seven months longer than the season for Fort Assinniboine, the immediate suggestion is that measuring seasonal evaporation only, and basing full year relationships thereon, cannot be justified. This suggestion is strengthened by the fact that the highest of the eight y/x ratios (outside of Fort Assinniboine and Hays), 1.33 at Denver and 1.35 at Lake Hefner, are also seasonal figures, while full-year comparisons at six of the eight yielded y/x ratios between 1.20 and 1.29.

On the possibility that May–September seasonal y/x factors would differ from those for full years or other seasons, a few were computed on the 5-month season basis for comparison. These are listed in table 4. Differences were found, but they are seen to be quite small. The figures serve to confirm that comparisons made in one section of

TABLE 4.—*Comparison of 5-month seasonal values of y/x with values for other periods*

Location	y/x	
	5-month period	Periods of other length
Fort Assinniboine, Mont.	1.46	
Hays, Kans.	1.45	1.46 (6 months).
Lake Hefner, Okla.	1.31	1.35 (annual).
Buchanan Dam, Tex.	1.19	1.20 (annual).
Lake Kickapoo, Tex.	1.27	1.30 (annual).

the nation are not necessarily representative of other areas, and that geographical (and associated) differences between locations are probably at least as important as seasonal considerations.

The difficulties in making accurate evaporation measurements are well known, and appear to have had their effects on the measurements at Fort Assinniboine. Such things as heavy rains splashing out or in, high winds splashing water out of one or both pans, setting micrometer gages under high wind conditions, and pans overflowing from heavy precipitation, all make comparative daily measurements difficult and will explain some of the daily evaporation variation between pans. Most of the variation seems due, however, to consistently lower daytime temperatures of the sunken pan. The only days on which the sunken pan had a warmer maximum temperature were those with rapid cooling of the atmosphere in the area, and the sunken pan, due to a larger mass of water and heat stored both in water and surrounding earth, was slower to cool. Comparative pan water temperatures are discussed in a later section. On the basis of these comparisons it appears that the y/x ratio experimentally determined at Fort Assinniboine has application only in areas limited to similar seasonal and possibly latitudinal conditions.

3. ANALYSIS OF CLASS A AND BPI EVAPORATION

In the preceding section May–September comparisons of Fort Assinniboine evaporation from the two types of pan appear to produce a rather high y/x ratio (1.46), even though the ratio agrees almost exactly with that for Hays, Kans., for a similar season. Full year experimental comparisions at other points show an annual ratio of about 1.25. It appeared possible, in view of this large difference, that Fort Assinniboine might experience a marked lowering of the y/x ratio during winter. The reasoning which suggests this possibility is that, during the warmer season of the year when air temperatures average warmer than soil temperatures, there would be some water heat loss through the sunken pan into the ground, particularly during the warmest period of each day. (Measurement of air and soil temperatures at the 20-inch depth at Bozeman, Mont. during summer months, shows that mean air temperature during summer runs 2° to 4° F. warmer than that of soil at the 20-inch depth—the depth of the bottom of the BPI pan. The same record shows that this temperature gradient reverses during the winter, with even greater differences.) At Silver Hill, Md., the Weather Bureau has found that insulating the BPI sunken pan against heat loss increases its evaporation 6 to 8 percent. On the other hand, during the colder months at Fort Assinniboine (not comparable at all with Silver Hill), *if* evaporation were measureable, much of the time heat traveling through the BPI pan from the ground through the water (or ice) to the air (reverse of warm season) could be expected to reduce the y/x ratio appreciably by keeping the sunken pan temperature warmer relative to the air than during the summer, and increasing its comparative evaporation as a result.

An attempt was made to show heat loss to the ground through the BPI pan by computing evaporation from that pan first by using air temperature, dew point, radiation, and average daily wind movement (table 5), and comparing these results with evaporation computed from water surface temperature instead of air temperature in Dalton's [4] equation

$$E=(e_o-e_a)\ (a+bu).$$

However, the results made it apparent that the equation developed from BPI data at Lake Hefner (where [1] gives $a=0.253$ and $b=0.004$), is not applicable to Fort Assinniboine. The author cannot find the reason (or reasons) for this but further study appears desirable. It may be that heat loss through the pan from air to ground may have been most significant during the warmest part of the day, when evaporation rates were highest, and air temperatures averaged some 6° to 8° F. warmer than BPI pan water. At night, when BPI pan minimums ran 8° to 10° F. warmer than air, such factors as air temperature, differences in air and water vapor pressure, radiation, and wind were all at levels contributing to lowest diurnal evaporation rates. This is discussed in the section which follows.

In table 5 are listed data used in computations, which are based upon Penman's [6] equation,

$$E=\frac{1}{\Delta+\gamma}\ (Q_n\Delta+\gamma E_a),$$

where Δ is the slope of the saturation vapor-pressure vs. temperature curve (de_s/dT) at air temperature T_a; E_a is the evaporation given by the aerodynamic equation, assuming water temperature (T_o) equal to air temperature; Q_n is the net radiant energy expressed in the same units as E; and γ is defined by the equation

$$R=\gamma\left(\frac{T_o-T_a}{e_o-e_a}\right)$$

in which R is Bowen's [7] dimensionless ratio. The application to Fort Assinniboine data follows exactly the procedures outlined in [5]; in fact, use of the graphs of [5] yields results varying insignificantly from the computations, although actual computations were made and are

TABLE 5.—*Analytical computation of Class A and BPI pan evaporation using Havre and Fort Assinniboine meteorological data, 1955–57*

1 Month	2 T_a	3 T_d	4 R	5 U_p	6 Computed Class A Evap.	7 Computed BPI Evap.	8 Ratio Class A BPI	9 Average 1955–57 Class A Pan Obs. Evap.	10 Pan Coeff. from Comp. Evap.	11 Pan Coeff. from Obs. Evap.
January	10.4	4.0	156	155	0.90	1.26	0.71			
February	16.9	9.3	250	185	1.28	1.61	.79			
March	29.3	17.7	381	179	2.98	2.87	1.04			
April	41.9	26.3	459	169	4.77	4.29	1.11			
May	55.6	37.6	517	147	7.46	5.83	1.28	7.95		
June	63.7	44.7	625	153	10.00	7.17	1.39	9.83		
July	70.7	49.7	624	133	11.36	7.97	1.42	11.61		
August	68.0	45.3	542	128	10.02	7.16	1.40	11.00		
September	57.1	38.3	405	124	6.19	4.86	1.27	5.89		
October	45.5	30.7	253	141	3.90	3.44	1.13			
November	27.6	17.0	152	166	2.04	2.04	1.00			
December	24.2	12.7	114	176	2.01	2.02	1.00			
May-September					45.03	32.99	1.36	46.28	.665	.647
Annual					62.91	50.52	1.25		.661	

T_a Average air temperature (°F.) 1955–57 for Havre, Mont.
T_d Average dew point (°F.) 1955–57 for Havre. (Values for Aug.–Dec. 1957 and Jan. 1955 estimated from surrounding stations.)
R Average radiation, Langleys/day (interpolated from Great Falls and Glasgow observed radiation).
U_p Average pan wind, mi./day (Fort Assinniboine Class A pan).

listed in table 5. The May–September y/x ratio, based upon computed evaporation, turns out to be 1.36, compared with 1.46 for the 8-year observed ratio. This 1.46 value was remarkably stable from year to year, suggesting the possible conclusion that computed BPI pan evaporation is too large, through not allowing for sufficient heat loss through the pan during the season of highest evaporation rates. This 1.36 value might be considered an estimate of what the season y/x ratio would be if the BPI pan were insulated, representing a possible increase of about 11 to 12 percent in evaporation from the sunken pan as compared with the 8 percent increase determined experimentally at Silver Hill.

Because the Class A pan seasonal coefficient was computed to be 0.665 (factor for yielding lake evaporation from Class A totals), while the coefficient from observed data was 0.647, it may be concluded that the analytical Class A computations produce results not significantly different from observed data. This has been the experience at Lake Hefner [1] and Lake Mead [8] for longer seasons, and leads to the assumption that the analytical computations for the full year at Fort Assinniboine are reasonably good. In the 6th and 7th columns of table 5 it is interesting to note that the computed evaporation from the BPI pan is larger than similar computations for the Class A pan during midwinter, and is about the same during early spring and late autumn. It is during midsummer that the Class A pan evaporates much more than the sunken unit, and because evaporation volume is the highest at about the same time the monthly y/x ratio is largest, the winter reversal of the y/x ratio has only a small effect on the annual totals. Table 5 covers only the 3 years for which data for the computation method were available, but since the y/x observed ratio varied within a range of less than 0.10 from year to year, any changes from computing for the entire 8-year period would necessarily be small.

It should be noted from this table 5 that temperature and dewpoint data from Havre (8 miles northeast of, and 200 ft. lower elevation than Fort Assinniboine) were used. Climatologically, these two places are not identical. Fort Assinniboine has much more wind than Havre, and the Havre temperature averages 1.3° F. warmer throughout the year. This use of Havre temperatures, because of their higher average than the evaporation pan location, tends to produce higher computed evaporation values than if suitable temperature data had been available for Fort Assinniboine. Havre dewpoints would also be expected to run higher than Fort Assinniboine's, and this factor would produce lower computed evaporation values. Further, Havre has a valley bottom location, Fort Assinniboine is on a relatively flat plain; Havre rainfall runs nearly 10 percent greater than at the Fort, and the Havre instrument site has less sunshine than Fort Assinniboine. The computed values, then, must be considered rough estimates and as an example of the analysis possible if suitable data were available. Their value is in providing evaporation loss estimates for the part of the year when measurements are impractical.

The seasonal (May–September) y/x computed ratio (column 8 of table 5), when compared with observed ra ios (table 1), reveals large differences in May and June (1.28 vs. 1.50; 1.39 vs. 1.46), two months when heat loss through the sunken pan should be large because rapidly warming atmosphere and much more slowly warming earth would produce a large heat gradient toward the ground. The large difference in September (1.27 vs. 1.42), although not as large as in May, is not easily explained, and probably reflects some of the limitations of the data used in the computations.

4. WATER (BOTH PANS) AND AIR COMPARATIVE TEMPERATURES

Tables 6–8 list monthly water temperature averages for the two pans. Although a leaking BPI pan destroyed evaporation comparisons during 1957, water temperature measurements were continued for both units until the end of September, yielding a fraction more than five seasons

TABLE 6.—*Comparison of WB Class A and BPI sunken evaporation pan temperatures, Fort Assinniboine, Montana*

Year	Average Pan Maximum Temperature									
	May		June		July		August		September	
	A	BPI	A	BPI	A	BPI	A	BPI	A	BPI
1952							78.6	74.8	70.9	67.2
1953	65.7	59.8	73.1	69.2	82.2	77.6	80.0	74.9	71.0	65.8
1954	69.4	62.8	71.7	65.6	84.1	77.2	78.4	74.2	69.2	64.6
1955	61.3	58.0	*67.7	66.8	*75.2	72.6	82.1	74.9	64.3	60.8
1956	64.9	60.8	76.9	71.1	*82.0	75.7	76.8	72.3	65.9	62.9
1957	*66.6	61.9	73.4	69.2	82.1	74.3	79.2	73.6	68.9	64.6
Total	327.9	303.3	362.8	341.9	405.6	377.4	475.1	444.7	410.2	385.9
Years	5	5	5	5	5	5	6	6	6	6
Average	65.6	60.7	72.6	68.4	81.1	75.5	79.2	74.1	68.4	64.3
Diff		4.9		4.1		5.6		5.1		4.1

*These values differ from those published in *Climatological Data* for a variety of reasons. In some cases data for one pan were not used here if data for the other were unobserved for any reason, and in others small errors have been found in the publication which are being corrected.

TABLE 7.—*Average pan minimum temperature*

Year	May		June		July		August		September	
	A	BPI	A	BPI	A	BPI	A	BPI	A	BPI
1952							52.6	60.3	45.5	52.6
1953	42.5	48.7	52.0	57.4	55.5	65.1	53.3	62.1	45.6	53.5
1954	44.4	51.6	49.4	56.2	56.8	65.4	56.8	62.4	46.7	53.9
1955	43.4	49.7	*50.7	59.6	57.0	63.5	53.8	62.5	*41.7	*50.0
1956	45.2	52.3	52.7	60.0	*56.4	64.0	53.8	60.1	44.9	52.0
1957	*47.0	52.9	53.9	59.8	56.7	59.8	54.7	61.2	45.6	51.6
Totals	222.5	255.2	258.7	293.0	282.4	317.8	325.0	368.6	270.0	313.6
Years	5	5	5	5	5	5	6	6	6	6
Average	44.5	51.0	51.7	58.6	56.5	63.6	54.2	61.4	45.0	52.3
Diff		6.5		5.9		7.1		7.2		7.3

*See note to Table 6.

TABLE 8.—*Average pan water temperature*

Year	May		June		July		August		September	
	A	BPI	A	BPI	A	BPI	A	BPI	A	BPI
1952							65.6	67.6	58.2	59.9
1953	54.1	54.3	62.6	63.3	68.9	71.4	66.7	68.5	58.3	58.7
1954	56.9	57.2	60.6	60.9	70.5	71.3	67.6	68.3	58.0	59.3
1955	52.4	53.9	59.2	63.2	66.1	68.0	68.0	68.7	53.0	55.4
1956	55.1	56.6	64.8	65.6	69.2	69.9	65.3	66.2	55.4	57.5
1957	56.8	57.4	64.7	64.5	69.4	67.1	67.0	67.4	57.3	58.1
Totals	275.3	278.4	310.9	317.5	344.1	347.7	401.2	406.7	340.2	348.9
Years	5	5	5	5	5	5	6	6	6	6
Average	55.1	55.9	62.2	63.5	68.8	69.5	66.9	67.8	56.7	58.2
Diff		0.8		1.4		0.7		0.9		1.5

of water temperature comparisons. In table 9 appear average air temperatures for the same periods.

Pan average maximum temperature (table 6) was rather consistently warmer from month to month in the Class A unit, although occasionally a day with rapid cooling of the weather in general would produce a higher sunken pan water temperature. This consistent pattern (27 months) seems to imply some actual heat loss from the sunken pan to the ground, at least during the warmest (and highest evaporation) part of the day, although a large part of the difference, of course, is caused by heat radiation on the sides of the Class A pan. In table 7, however, we

TABLE 9.—*Average air temperature, Fort Assinniboine*

Year	May	June	July	August	September
		Maximum			
1952				84.1	76.2
1953	61.7	70.3	84.1	86.1	75.1
1954	63.9	70.5	87.1	78.6	68.7
1955	62.3	73.5	78.0	86.0	69.6
1956	65.6	78.9	83.0	80.6	71.3
1957	71.5	74.3	88.8	81.5	71.3
Average	65.0	73.5	84.2	82.8	72.0
Class A Average	65.6	72.5	81.1	79.2	68.4
BPI Average	60.7	68.4	75.5	74.1	64.3
		Minimum			
1952				49.7	45.0
1953	38.1	48.1	53.6	51.9	44.2
1954	39.2	48.0	55.9	54.4	44.5
1955	40.2	47.5	54.5	50.9	39.9
1956	41.9	51.1	53.9	51.2	43.2
1957	41.8	48.7	55.4	52.7	43.5
Average	40.2	48.7	54.7	51.8	43.4
Class A Average	44.5	51.7	56.5	54.2	45.0
BPI Average	51.0	58.6	63.6	61.4	52.3
		Mean			
1952				66.9	60.6
1953	49.9	59.2	68.9	69.0	59.7
1954	51.6	59.3	71.5	66.5	56.6
1955	51.3	60.5	66.3	68.5	54.8
1956	53.8	65.0	68.5	65.9	57.3
1957	56.7	61.5	72.1	67.1	57.4
Average	52.7	61.1	69.5	67.3	57.7
Class A Average	55.1	62.1	68.8	66.9	56.7
BPI Average	55.9	63.5	69.5	67.8	58.2

find that the pattern reverses; the sunken pan had consistently warmer minimums except for an occasional day when a marked warming covered the area, warming the Class A unit more rapidly than the other. Because the BPI unit was warmer only during the portion of the day with lowest overall evaporation rate (night), it may be assumed that even though the BPI pan might have a higher nighttime evaporation rate than the Class A, this effect must be more than offset by the increased Class A ratio during the heat of the day, caused by higher temperatures, possible wind differences, and other diurnal factors. A brief experiment with sunrise and sunset readings for part of a summer season seems to be suggested.

For the average overall temperature for both units, the BPI pan ran about 1.2° F. warmer than the Class A. The result must be considered along with duration of day and night during the season sampled. During June the period between sunset and sunrise lasts only 8 to 9 hours, and only for a portion of that period would the Class A water be cooler than the sunken pan water. With sunlight lasting 15 to 16 hours, and with the Class A water warming quickly after sunrise, it seems evident that the Class A water temperature would normally be the warmer of the two for at least 14 hours of each day. This could be tested by a short period of hourly observations (a month or so), or by distant recording thermographs with temperature elements immersed in the water.

Table 9 lists average air temperatures, with water temperatures for the two pans included for convenience in comparison. It is interesting to note that sunken pan temperatures compare more closely with air average

means; they average much warmer than air in the average minimum category; but in the very important average maximum category, sunken pan water temperature averages much cooler. The water average maximum temperature for the Class A pan runs slightly cooler than that for air, probably due to evaporational cooling during the warmest part of the day. In another experiment of this kind it would be well to develop characteristic daily temperature curves for air and Class A and BPI water. The Fort Assinniboine results suggest that computing daily average water temperatures on the same basis (maximum plus minimum divided by 2) as for air, may be worth experimental study to determine its validity as a practice.

5. REPRESENTATIVENESS OF DATA

Table 10 lists comparative Class A evaporation figures as available in North Central Montana for the period the two pans were compared at Fort Assinniboine. A question arose as to whether Class A evaporation at that point was too high and not representative for an area. Tiber Dam, situated about 75 miles west-southwest of Fort Assinniboine, during the eight years of comparison came very close to Assinniboine totals in five years. Malta, in the bottom of the Milk River Valley, showed much less evaporation, but there the pan is in an area of much less wind movement and of somewhat higher relative humidity. Considering the Fort Assinniboine exposure along with results listed in table 10 for Tiber Dam, data from each seem to support the other, and probably indicate that while Fort Assinniboine seasonal evaporation may be high, and may be near the maximum for the area it represents, it still represents a large (perhaps as much as 3,500 sq. mi.) section of plateau country between the Milk and Marias River Valleys (Tiber Dam is on the Marias River). Reference to figure 1 will show the type of level plateau on which Fort Assinniboine is located.

TABLE 10.—*Seasonal evaporation, North Central Montana, WB Class A installations (May–September, incl.)*

Year	Fort Assinniboine	Tiber Dam	Malta	Lonesome Lake
1949	55.45	52.99	33.41	49.05
1950	42.28	39.47	26.22	----------
1951	42.11	42.06	----------	37.87
1952	50.58	47.03	27.63	37.54
1953	45.44	41.55	28.98	37.89
1954	43.49	38.17	21.95	----------
1955	42.85	36.75	27.26	----------
1956	48.48	36.79	----------	----------

ACKNOWLEDGMENTS

Thanks are due Messrs. Nordenson and Baker of the U.S. Weather Bureau's Hydrologic Services Division in Washington, D.C. for their help on the analytical comparisons; to M. D. Magnuson, Area Climatologist, U.S. Weather Bureau, Seattle, for help on organizing details; and to the several Superintendents of the North Montana Branch Experiment Station at Fort Assinniboine, without whose work and cooperation this report would not be possible.

REFERENCES

1. Max A. Kohler, "Lake and Pan Evaporation," p. 131, *Geological Survey Circular* 229, "Water Loss Investigations: Vol. 1—Lake Hefner Studies Technical Report," Washington, D.C., 1952, pp. 127–148.
2. R. A. Dightman, "Comparison of the Evaporation Rate from WB Class A and USDA BPI Evaporation Pans," *Proceedings*, Montana Academy of Sciences, vol. 13, 1953, pp. 49–51.
3. Paul Brown and A. L. Hallstead, "Comparison of Evaporation Data from Standard WB and BPI Evaporation Pans," *Agronomy Journal*, vol. 44, No. 2, 1952, pp. 100–101.
4. V. Dalton, "Experimental Essays . . .", *Memoirs*, Manchester Literary and Philosophical Society, Series 1, vol. 5, Part 2, 1802, pp. 535–602.
5. Max A. Kohler, T. J. Nordenson, and W. E. Fox, "Evaporation from Pans and Lakes," Weather Bureau *Research Paper* No. 38, May 1955, 21 pp.
6. H. L. Penman, "Natural Evaporation from Open Water, Bare Soil, and Grass," *Proceedings*, Royal Society of London, Ser. A, vol. 193, No. 1032, Apr. 1948, pp. 120–145,
7. I. S. Bowen, "The Ratio of Heat Losses by Conduction and by Evaporation from Any Water Surface," *Physical Review*, Ser. 2, vol. 27, June 1926, pp. 779–787.
8. G. Earl Harbeck, Jr., et al., "Water Loss Investigations:—Lake Mead Studies," U.S. Geological Survey *Professional Paper* 298, Washington, D.C. 1958, 100 pp.

Weather Note

TWO UNIQUE EASTERN PACIFIC HURRICANES OF 1957

RUE E. RUSH

Weather Bureau Airport Station, Honolulu, Hawaii

[Manuscript received March 18, 1959; revised March 21, 1960]

1. INTRODUCTION

Most storms forming in the area southwest of Manzanillo, Mexico begin moving westward, but quickly recurve, move northward, lose their tropical identity, and fill rapidly. A few, with a higher energy level than usual, or supplemented by extratropical systems to the north, move far enough to the north to bring rain, and less often, high winds to southern California. Others curve to the northeast and move toward or into Mexico until they dissipate. At least one crossed into the Gulf of Mexico [1], moved over that body of water, and reached Florida. A very few do not recurve at all, but continue a general westward movement. In 1957 two of these latter progressed far beyond the normal paths.

This paper attempts to analyze these storms, in some measure to explain the reasons for westward movement, and to evaluate conditions which caused the early demise of the first, Kanoa, and the intensification of the second at a latitude where normally a change to extratropical type of storm would be expected.

Analysis and evaluation were severely limited by lack of data. Unlike the Caribbean-Atlantic and the western Pacific areas where many previous studies have been made on tropical storms, the area between Hawaii and Mexico is completely without upper air data and virtually without surface data. These limitations preclude accurate application of suggested forecast techniques for long periods in the lives of the storms, or may even rule out an approach completely. An example of this is clearly shown in the case of Kanoa, where the Riehl-Haggard [2] method was inapplicable because the southern part of the grid extended into an area where even normal height charts are subject to suspicion.

2. THE FIRST STORM, KANOA

Kanoa was first recognized in a bulletin issued by the San Francisco Weather Bureau office at 0700 GMT, July 15, 1957. The bulletin, based largely on a report from the ship *Gravel Park*, which reported a westerly wind of 45 knots and a pressure of 998 mb. at 2000 GMT, July 14, placed the center about 750 miles southwest of Manzanillo, Mexico. The San Francisco office continued issuing bulletins until 0900 GMT, July 18, when lack of data forced abandonment.

However, three days later, at 0300 GMT, July 21, the ship *Cape Horn*, located near 15° N., 130° W., reported 67 m.p.h. winds and very high seas with precipitous swells. On receipt of this information, the San Francisco office resumed issuance of advisories, now raising the storm into the hurricane category. The *Cape Horn* remained either in or on the periphery of the storm for the following four days, rendering invaluable aid in charting the course and intensity of the storm.

On July 22, a plane from the 57th Weather Reconnaissance Squadron, Hickam Air Force Base, Oahu, located the eye, about 40 mi. in diameter, and estimated the maximum sustained winds to be 70 kt. with gusts to 100 kt. The next day the ship *Elba* added reports that were extremely helpful in the analysis of the situation. The Air Force reconnaissance continued daily until the storm filled and winds dropped below 35 kt.

Normally, data southeast of Hawaii are conspicuous by their virtual absence. In this case, though, Kanoa travelled almost the same path as the shipping lane between Hawaii and the Canal Zone. This coincidence provided enough data to allow excellent results in forecasting movement and character of the storm.

As the storm neared the 140th meridian, the Weather Bureau office in San Francisco transferred responsibility for issuance of advisories to the Weather Bureau in Honolulu. The Hawaiian military meteorological offices, responsible for slightly different areas than the Weather Bureau, had already begun issuing their warnings, and had named the storm Kanoa, a Hawaiian word meaning loosely "the free one."

As Kanoa approached the 145th meridian, it became apparent that there would be little or no chance for recurvature as the semipermanent Pacific High was strengthening to the north, and ridging farther westward (figs. 1, 2). This formed an effective block, such as is suggested by Simpson [3], at least in the lower layers. Aloft, a Low formed just to the northeast of the Islands, and was later reinforced by colder air from a trough

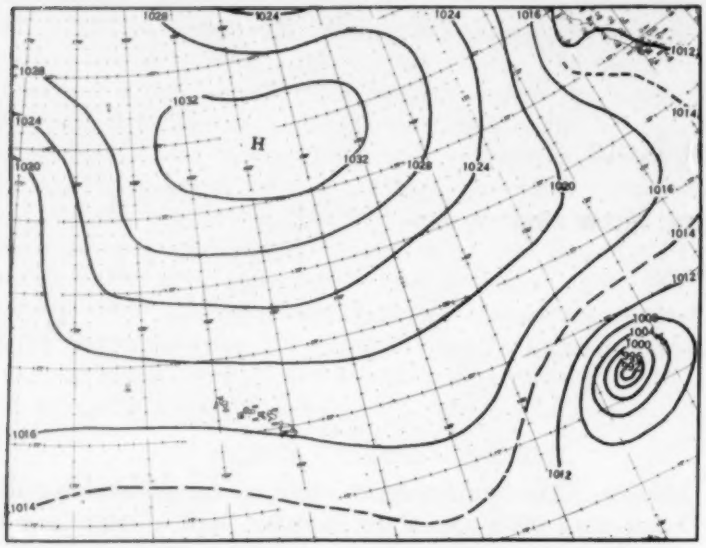

FIGURE 1.—Sea level pressure (mb.), 1200 GMT, July 21, 1957.

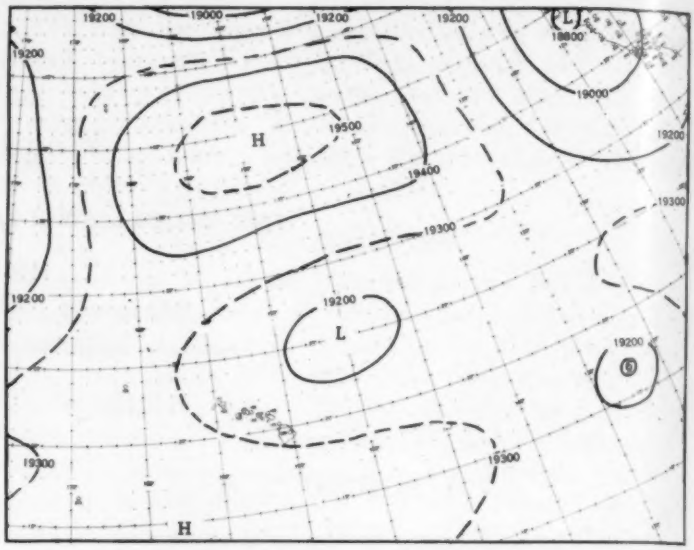

FIGURE 3.—500-mb. height (ft.), 1200 GMT, July 21, 1957.

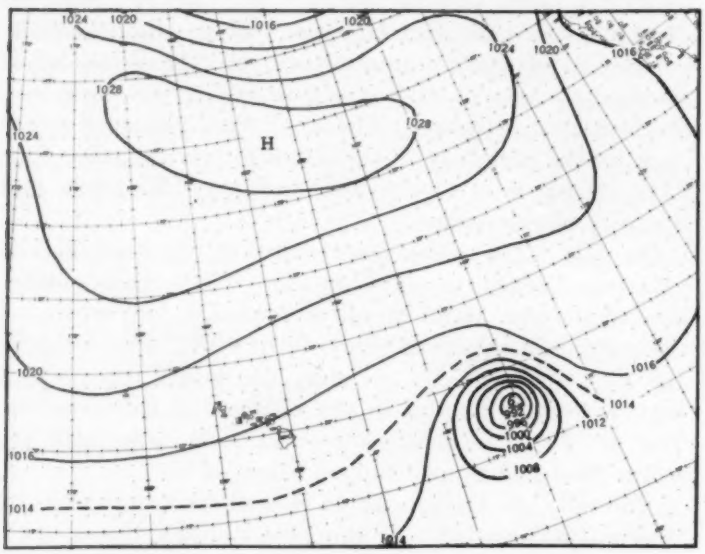

FIGURE 2.—Sea level pressure (mb.), 1200 GMT, July 23, 1957.

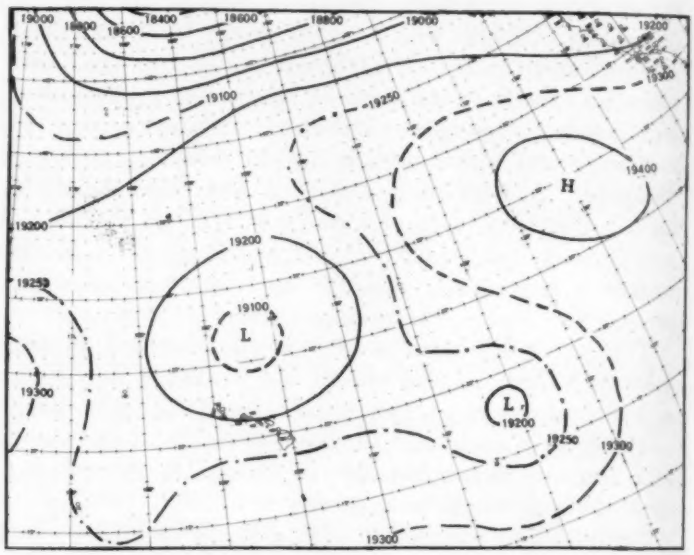

FIGURE 4.—500-mb. height (ft.), 1200 GMT, July 23, 1957.

extending southwestward from the vicinity of the Aleutians (figs. 3, 4). With the lower-level pattern forcing Kanoa to remain on a track with a westward component, but with the upper air picture suggesting that colder air would alter the characteristics of the tropical storm, the life of Kanoa as a hurricane was doomed. It weakened steadily, and the portion above 10,000 ft. or so was incorporated into the cold trough. By July 23, the storm at 700 mb. was part of a broad trough in the easterlies which had several lesser but distinct closed circulations (fig. 5). The part below 10,000 ft. continued its westward movement, filling rapidly. By the time it had reached the Hawaiian Islands, it was little more than a perturbation in the easterly flow (fig. 6). However, it caused a marked increase in rainfall over Hawaii, though the rain fell in a nearly normal trade wind pattern. A less pronounced increase in surface winds was also observed.

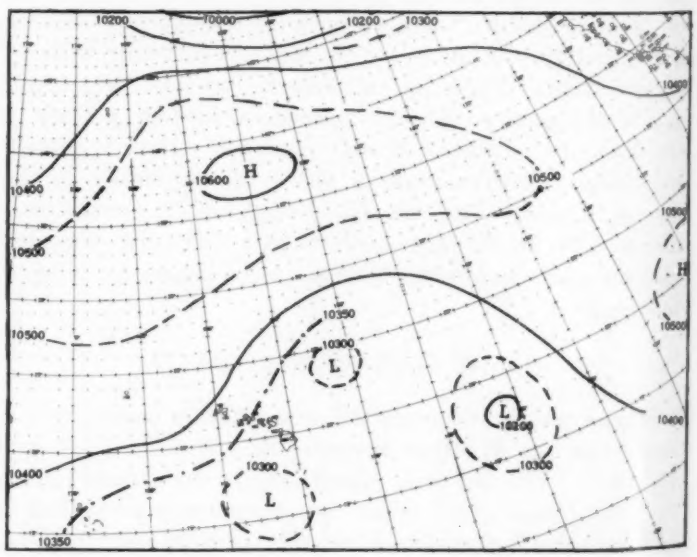

FIGURE 5.—700-mb. height (ft.), 1200 GMT, July 23, 1957.

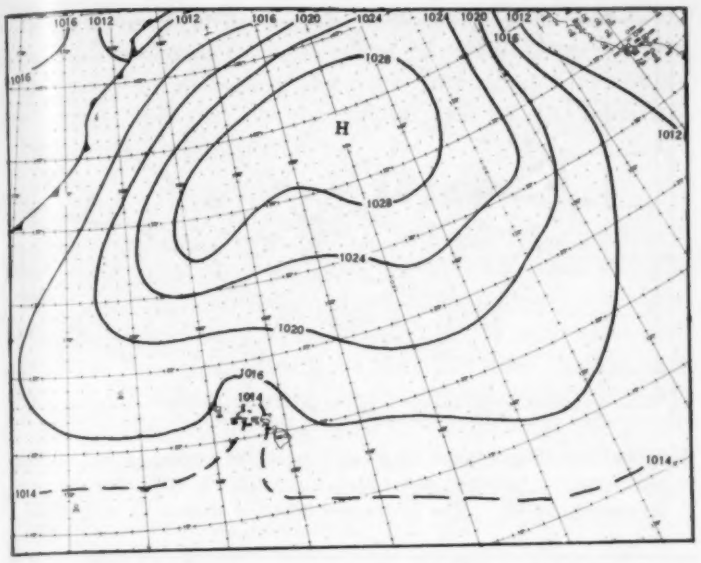

FIGURE 6.—Sea level pressure (mb.), 1200 GMT, July 26, 1957.

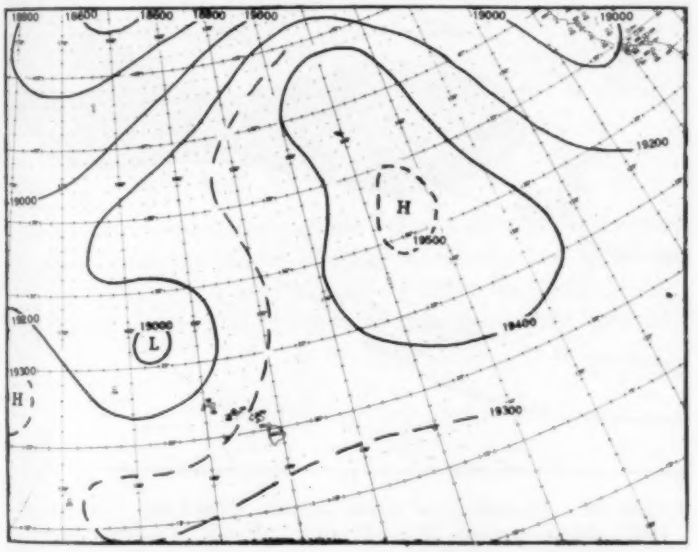

FIGURE 7.—500-mb. height (ft.), 1200 GMT, July 26, 1957.

Meanwhile, at the 500-mb. level, the circulation of Kanoa had been absorbed by the large cold Low so well that little or no evidence of Kanoa's existence remained (fig. 7).

Among the more interesting features of this storm was the regularity of movement which it exhibited. In its early stages, it moved at about 8 m.p.h. and accelerated slowly to about 12 m.p.h. and continued at that speed throughout the rest of its existence.

An attempted analysis of sea surface temperatures suggested by [4] was abandoned because no data were available.

3. THE SECOND STORM

HISTORY

About two weeks following Kanoa another tropical disturbance formed in roughly the same area, and crossed

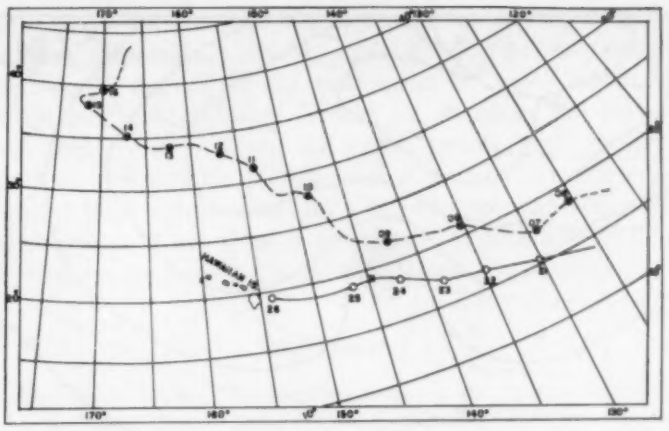

FIGURE 8.—Tracks of the two storms: Kanoa, July 21–26, 1957, solid lines; the unnamed storm, August 6–16, 1957, dashed lines. Positions are for 0000 GMT.

the 135th meridian at about 21° N., some 250 mi. north of Kanoa's crossing of this line. From this meridian movements of both storms were parallel for the next 600 mi., each progressing slightly north of west.

Somewhere near the 145th meridian, this second storm turned sharply to the north-northwest and accelerated for a 12-hour period (fig. 8). From analysis of charts during this period, it appeared that cold air had entered the vortex of the storm, and that it was rapidly becoming extratropical. As it crossed the flight path of Hawaii-California planes during this period, revisions of flight forecasts were necessary due to rapid and significant changes in both flight weather and winds. Winds reported by aircraft increased in speed with height in the atmosphere, so this lent support to the analysis that the storm was becoming extratropical. Certain analysis was impossible because necessary data were not available; however, after this relatively short period, the storm again slowed down, and there was considerable evidence (notably winds and temperatures reported by the Air Force reconnaissance plane which surveyed the storm) either that it had regenerated or that previous analyses had been in error. The storm was very small, since surface craft no more than 100 mi. from the eye reported no winds over 25 kt., and no adverse weather. Twenty-four hours after the deceleration began, the storm had intensified into a full-fledged hurricane (fig. 9).

For the next four days the storm maintained hurricane strength, and moved in a general northwestward direction. The maximum reported surface wind occured at 35.3° N., 166.5° W. at 1800 GMT, August 13 (fig. 10); the ship *Jean Lafitte*, apparently passing very near the center, reported a southerly wind of 90 kt. and surface pressure of 999 mb. It was not until the storm had reached a latitude of about 38° N. that it lost its tropical characteristics and moved rapidly away to the northeast (fig. 11).

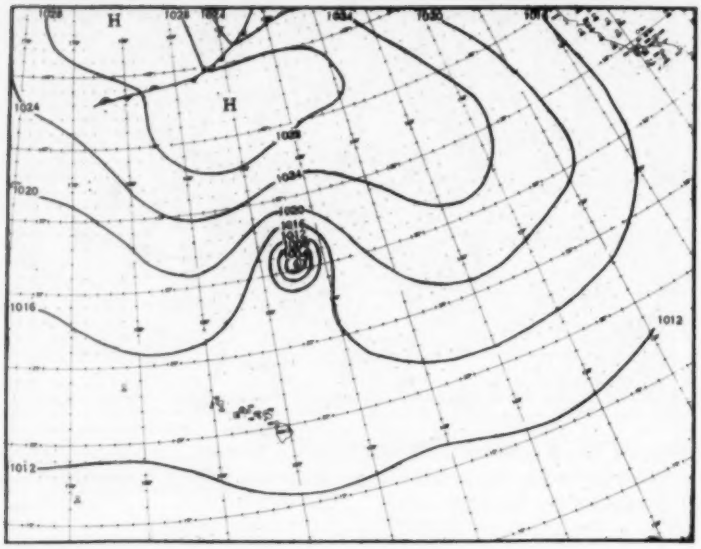

FIGURE 9.—Sea level pressure (mb.), 1800 GMT, August 10, 1957.

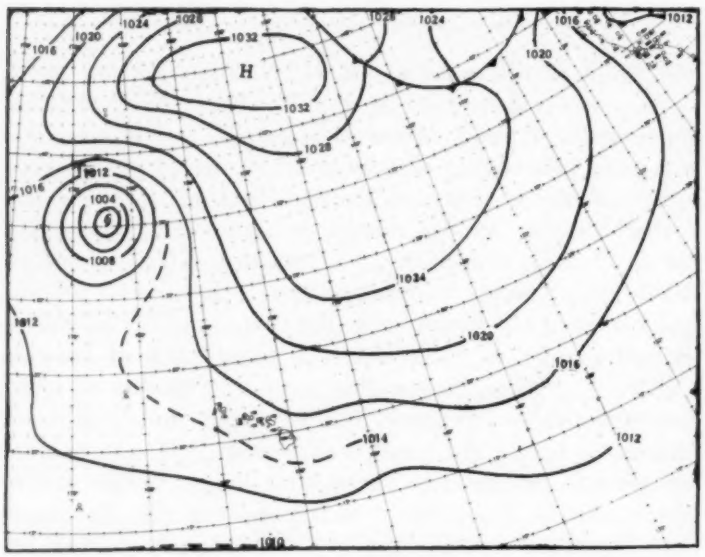

FIGURE 10.—Sea level pressure (mb.), 1800 GMT, August 13, 1957.

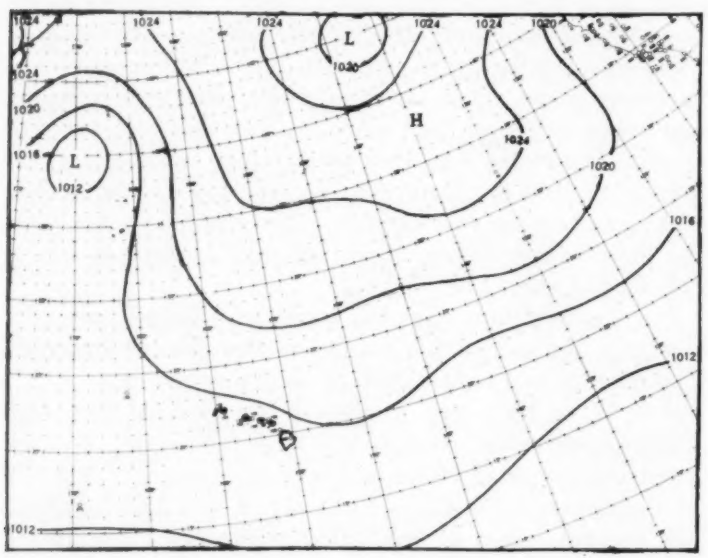

FIGURE 11.—Sea level pressure (mb.), 1800 GMT, August 15, 1957.

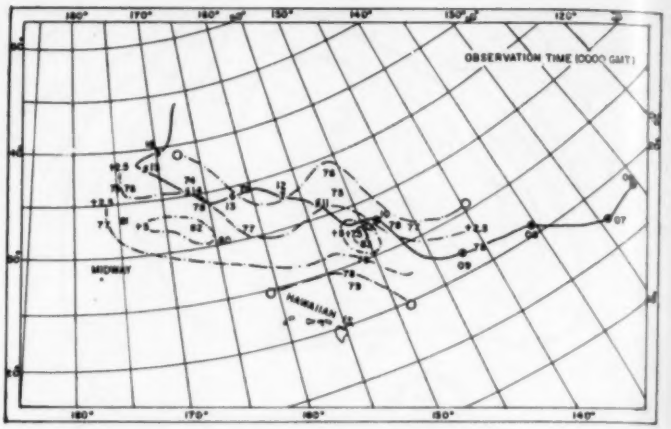

FIGURE 12.—Departures (dash-dot lines) of reported sea surface temperatures (plotted numbers), August 5–18, 1957, from normal temperatures [5]. The hurricane track is shown by solid line.

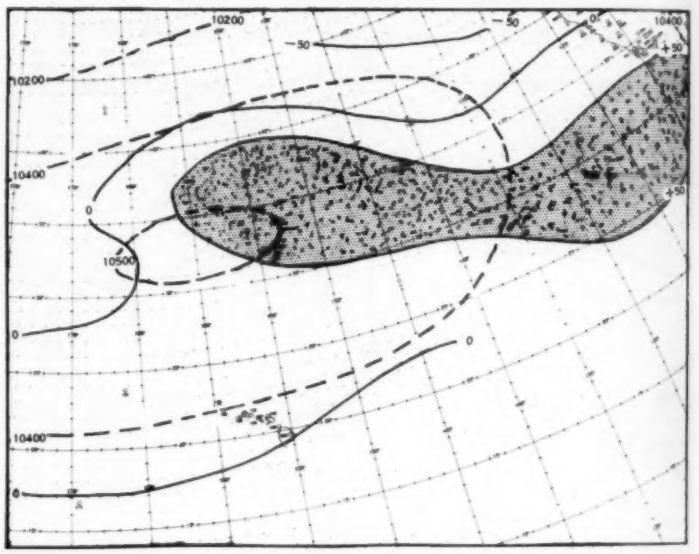

FIGURE 13.—Departure of mean 700-mb. height for July–August 1957 from normal July–August 700-mb. height. Normal heights are dashed lines, departures from normal, solid lines. Shaded area represents positive departure greater than 50 ft.

SEA SURFACE TEMPERATURE FIELD

Since this storm passed over shipping lanes between the west coast of North America and Hawaii and also between Japan and the United States, enough surface data were obtained for a good analysis of the sea surface temperature field. Sea surface temperatures received during the period from August 5 to 18 were plotted and compared with normals [5] for the month of August (fig. 12).

It appears that the extremely high sea surface temperatures in the area may have been related to deceleration, intensification, and direction of movement of the storm. The maximum deviation from normal temperature occurred in the direction of movement of the storm (fig. 12), and

the storm reached hurricane intensity after it had been near this maximum for a period of 12 to 18 hours. So far as existing data indicated, the storm's movement seemed to be roughly parallel to the major axis of the positive temperature anomaly field.

COMPARISON WITH NORMALS

Comparing the mean 700-mb. chart for the months of July and August 1957 with the normals for those months showed that the height anomaly was considerably positive from 22° N. to 35° N. from about 135 °W. eastward into the North American continent, and that the Pacific high cell north of Hawaii was larger than normal and displaced to the east (fig. 13). The normal north-south trough off the west coast of California and Mexico was damped markedly, and a narrow but definite east-west ridge appeared, extending from southern Arizona through northern Baja California, to a point near 28° N., 125° W., then curving northwestward to the high cell northeast of Hawaii. These deviations from normal suggest a change in steering of storms originating during the period: the existing wedge steered the storm on a westward course instead of the more common recurving path northward along the trough line.

4. CONCLUSIONS

The set of conditions which force westward movement beyond the early stages of tropical storms in the eastern North Pacific is so rare that the chance for study of such storms is almost nil. From the meager facts presently available, it appears that the upper air anomalies along the 28th to 32d parallels, and especially the filling of the normal north-south trough off the west coast of North America, are strong contributing factors in causing the initial westward thrust. After the storm passes the area normally most favorable for northward recurvature, the subtropical High seems to act as a steering mechanism, until such time as other factors overcome the strength of this steering wedge and either cause or allow recurvature.

REFERENCES

1. Stephen S. Visher, "Tropical Cyclones in the Northeast Pacific Between Hawaii and Mexico," *Monthly Weather Review*, vol. 50, No. 6, June 1922, pp. 295–297.
2. H. Riehl and W. H. Haggard, "Prediction of Tropical Cyclone Tracks," Second Research Report, Task 12, U.S. Navy Bureau of Aeronautics, Project AROWA, 1953, 40 pp.
3. Robert H. Simpson, "On the Movement of Tropical Cyclones," *Transactions of the American Geophysical Union*, vol. 27, No. 5, Oct. 1946, pp. 641–655.
4. E. L. Fisher, "Part I, Hurricanes and the Sea Surface Temperature Field; Part II, The Exchange of Energy Between the Sea and the Atmosphere in Relation to Hurricane Behavior," *National Hurricane Research Project Report* No. 8, Washington, D.C., June 1957, 46 pp.
5. U.S. Navy, *Marine Climatic Atlas of the World*, Vol. II, The North Pacific Ocean, NAVAER 50–1C–529, 1956.
6. William T. Chapman, Jr. and Young T. Sloan, "The Paths of Hurricanes Connie and Diane," *Monthly Weather Review*, vol. 83, No. 8, Aug. 1955, pp. 171–180.
7. R. C. Gentry, "Forecasting the Formation and Movement of the Cedar Keys Hurricane, September 1–7, 1950," *Monthly Weather Review*, vol. 79, No. 6, June 1951, pp. 107–115.

THE WEATHER AND CIRCULATION OF MARCH 1960

A Cold, Snowy Month

CARLOS R. DUNN

Extended Forecast Section, U.S. Weather Bureau, Washington, D.C.

1. HIGHLIGHTS

Cold and snowy weather prevailed in the eastern two-thirds of the United States during March 1960, while temperatures in most of the remaining (western) portions were warmer than normal. Many of the eastern stations reported the coldest March of record, and in some places the monthly mean temperature was as much as 6° or 7° F. colder than the previous record low.

This prolonged wintry weather was associated with blocking in North America, which originated during the winter [10] and continued to dominate the circulation throughout most of March 1960. This block was so tenacious and widespread that the index of 5-day mean zonal westerlies for the temperate zone (35° N.–55° N.) averaged over the Western Hemisphere was continuously below normal from January 7–11, 1960 to March 19–23, 1960.

2. MEAN CIRCULATION

The monthly mean circulation at 700 mb. for March 1960 in the United States consisted of a ridge over the Plateau States and a pronounced trough along the east coast with an anomalous, northerly flow in between (fig. 1). The trough was associated with equatorward-displaced westerlies and cyclonic activity south of the blocking ridge centered over the Ungava Peninsula in eastern Canada. This ridge was abnormally cold and consequently not very impressive at the 700-mb. level where heights averaged only 160 feet above normal.

Blocking was also evident in other areas. High-latitude anticyclones with major positive anomalies were located in northeastern Siberia and in Scandinavia. In the eastern Atlantic the normal seat of cyclonic activity was displaced southward (note −350-ft. anomaly in fig. 1), and many storms were deflected by the blocking High into southern Europe. East of the Scandinavian High a much stronger than normal northerly flow produced unusually cold weather in central Eurasia.

A Gulf of Alaska Low appeared in the mean in March after being absent in January and February 1960. It was the southeastern component of the typical "omega" block in this region.

These 700-mb. centers of action also appeared on the sea level 30-day mean (fig. 2). As expected, the cold North American block was more prominent at the lower level; above normal pressures were observed over most of Canada and the United States, with a ridge extending from the Yukon to Florida. This sea level map is typical of those associated with cold regimes in eastern United States. In fact, the sea level mean for this March is similar to the one for March 1915 when many previous temperature records were established.

3. CHANGE IN MEAN CIRCULATION FROM FEBRUARY TO MARCH 1960

The major change in the mean circulation at 700 mb. from February to March was the diminution of blocking and above normal heights over Greenland and eastern Canada (fig. 3). The maximum anomalous height fall (−660 ft.) was centered over southern Greenland, but 700-mb. heights also fell over practically all areas of Canada. In the United States rises in the west combined with falls in the east to intensify the northwesterly flow in the eastern portion of the country. This resulted in a marked cooling in New England where monthly mean temperatures were actually colder in March than in February.

The intensity and evolution of the North American blocking is well illustrated by a time series of 5-day mean 700-mb. height anomalies which are two weeks apart (fig. 4). Heights were far above normal in eastern Canada during the middle of February. They fell slowly thereafter but were still 550 ft. above normal by mid-March. Subsequently, this blocking weakened and heights dropped to approximately 500 ft. below normal by the end of the month.

While the positive anomalies existed in eastern Canada, heights were subnormal to the south over the United States in a fashion quite typical of blocking. As the blocking relaxed, in late March, 700-mb. 5-day mean heights over eastern United States increased to above normal values for the first time since early February.

A simple index was computed to indicate further the persistence, early period strength, and gradual decline of blocking in eastern North America. This blocking index (fig. 5) was obtained by subtracting the 700-mb. 5-day mean height departures from normal averaged over a small area (10° square) centered at 35° N., 65° W. from

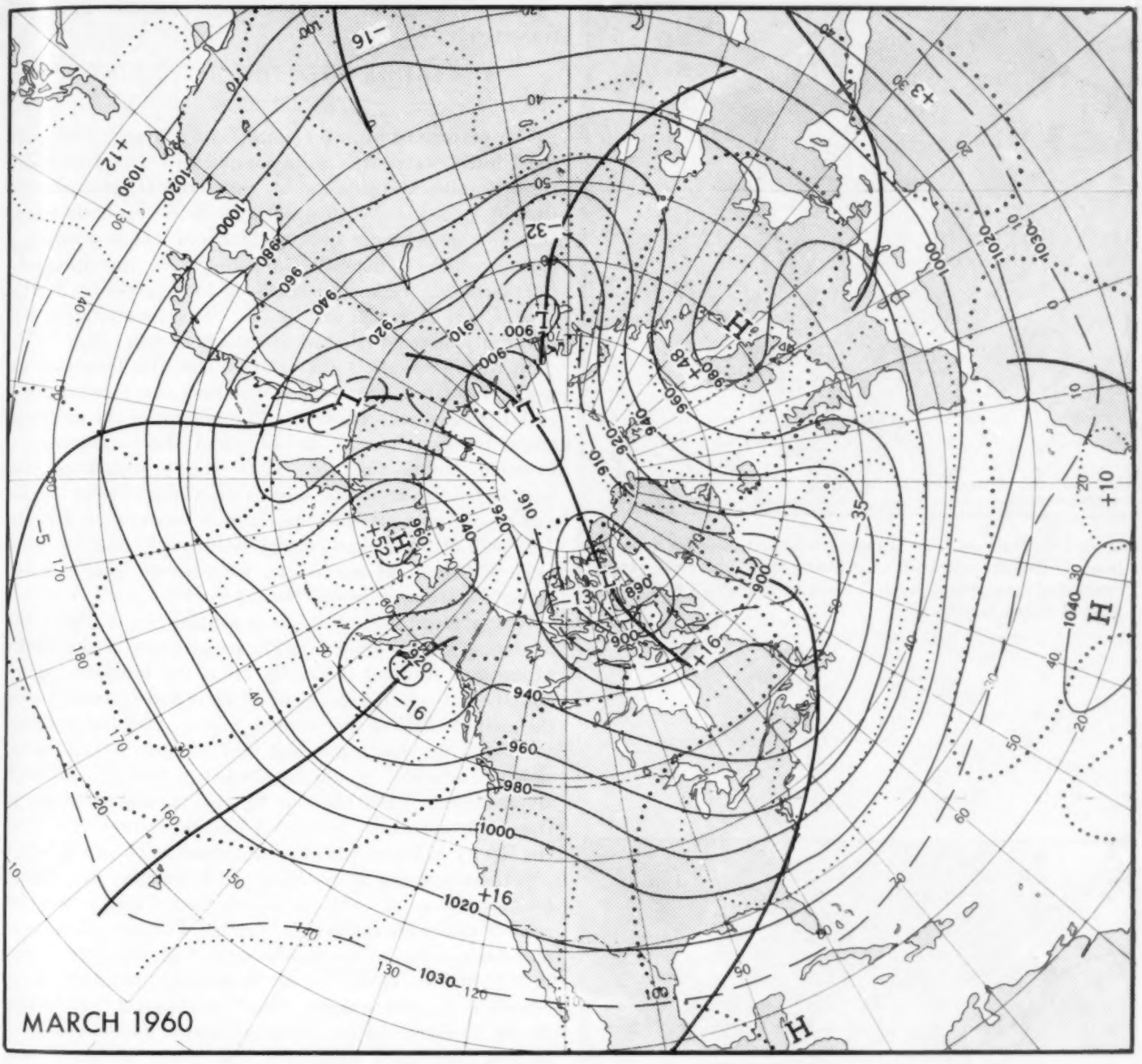

FIGURE 1.—Mean 700-mb. contours (solid) and height departures from normal (dotted), both in tens of feet, for March 1960. Blocking was prevalent this March.

a similar spatially averaged center at 60° N., 65° W. If height anomalies were more positive or less negative in the northern than in the southern area, this blocking index would be positive. A positive value also means, of course, that the westerlies were weaker than normal in this small longitudinal sector. Values were computed three times per week.

The blocking index was largest early in the period and continuously positive until the March 22–26, 1960 period. The decrease in blocking was gradual with only minor oscillations.

While blocking remained in eastern North America, surges of rising heights at high latitudes and falling heights at low latitudes migrated simultaneously westward, in a fashion referred to as a blocking surge by Namias [6]. By the first of March, 700-mb. heights were above normal in high latitudes from Greenland westward to eastern Siberia and generally subnormal in middle latitudes from Great Britain to the central Pacific (fig. 4). This regime changed slowly so that by the end of March the anomaly pattern had almost completely reversed with subnormal and

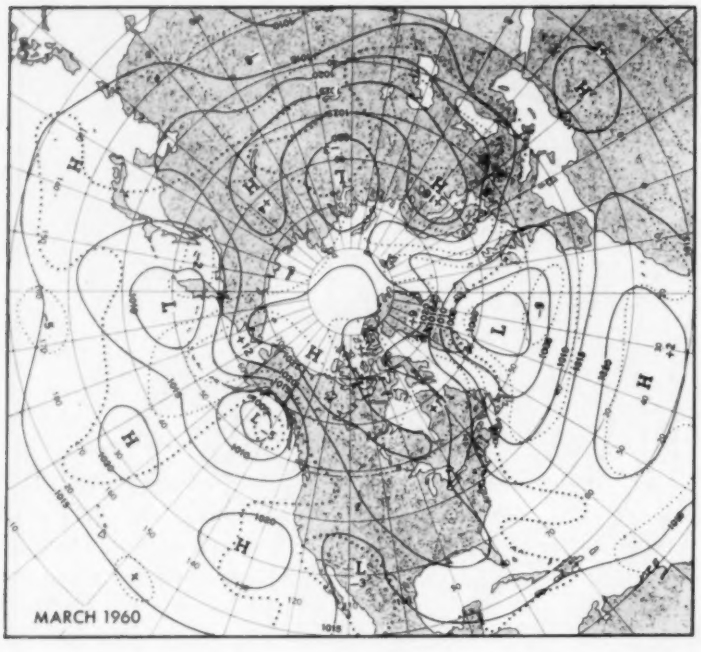

FIGURE 2.—Mean sea level isobars (solid) and pressure departure from normal (dotted), both in millibars, for March 1960. Isoline interval of anomalies is 4 mb. Pressure was above normal over most of North America.

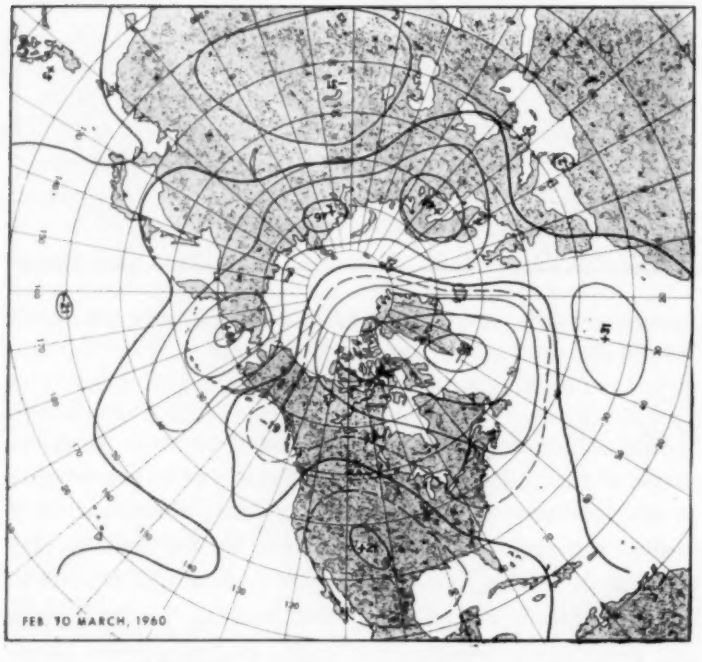

FIGURE 3.—Difference between monthly mean 700-mb. height anomaly for February and March 1960 (March minus February) in tens of feet. There were large height falls over eastern Canada and northeastern United States.

supernormal heights found in high and low latitudes, respectively.

4. WEATHER OVER THE UNITED STATES

PRECIPITATION

The pattern of total precipitation for March 1960 over the United States was quite complicated with essentially three small-scale patches of supernormal precipitation (fig. 6). In the Northwest the mid-tropospheric winds (fig. 1) were stronger than normal from the southwest, a factor which enhanced the orographic precipitation. Furthermore, there was some cyclonic activity in this area (Chart X in [12] and fig. 2). This precipitation was uniformly distributed throughout the month [13].

In the Southeast the circulation was also favorable for heavy rainfall. This region was near the mean trough, and depressed jet stream (fig. 1), near one of the preferred storm tracks (Chart X in [12]), and also in the area of frequent fronts (fig. 7). Here the precipitation was heavier than in any other part of the United States (fig. 6), and record amounts for March were reported in Florida. The bulk of this record rainfall occurred during the third week of March in connection with severe local weather along a stationary front (No. 12 in [13]).

Heavy precipitation over the central Great Plains and moderate precipitation in other regions east of the Rocky Mountains resulted indirectly from the blocking regime and the attendant cold mass of air which persisted over the eastern half of the United States. Several cyclones formed in the Southwest and Gulf of Mexico and moved slowly eastward or northeastward (Chart X in [12]). Overrunning of the obstructing cold airmass in front of these perturbations produced severe snowstorms from the Rocky Mountains to the east coast. The areas which experienced major snowstorms can be roughly determined by inspection of table 1 which lists various snowfall records that were made this March. Further information and descriptions of the snowstorms of March 1960 appear in [13], and in [4] there is an interesting discussion of the March 3–5, 1960 storm. This "northeaster," embedded in the blocking regime of early March, decelerated as it moved northward along the east coast of the United States and produced a great snowstorm in southeastern New England.

TABLE 1.—*Total snowfall for March 1960 at selected cities that received the largest amount for any March on record*

Station	Snowfall (in.)	Station	Snowfall (in.)
St. Joseph, Mo.	23.1	Harrisburg, Pa.	22.6
Columbia, Mo.	24.5	Roanoke, Va.	*30.3
Cairo, Ill.	20.3	Richmond, Va.	19.7
South Bend, Ind.	33.9	Asheville, N.C.	*28.9
Evansville, Ind.	20.2	Cape Hatteras, N.C.	8.5
Louisville, Ky.	22.9	Charlotte, N.C.	19.3
Lexington, Ky.	17.7	Greensboro, N.C.	*21.3
Knoxville, Tenn.	20.2	Greenville, S.C.	15.3
Akron, Ohio	20.9	Atlanta, Ga.	4.8
Youngstown, Ohio	20.6	Rome, Ga.	8.3
Pittsburgh, Pa.	21.3		

*Record for any month.

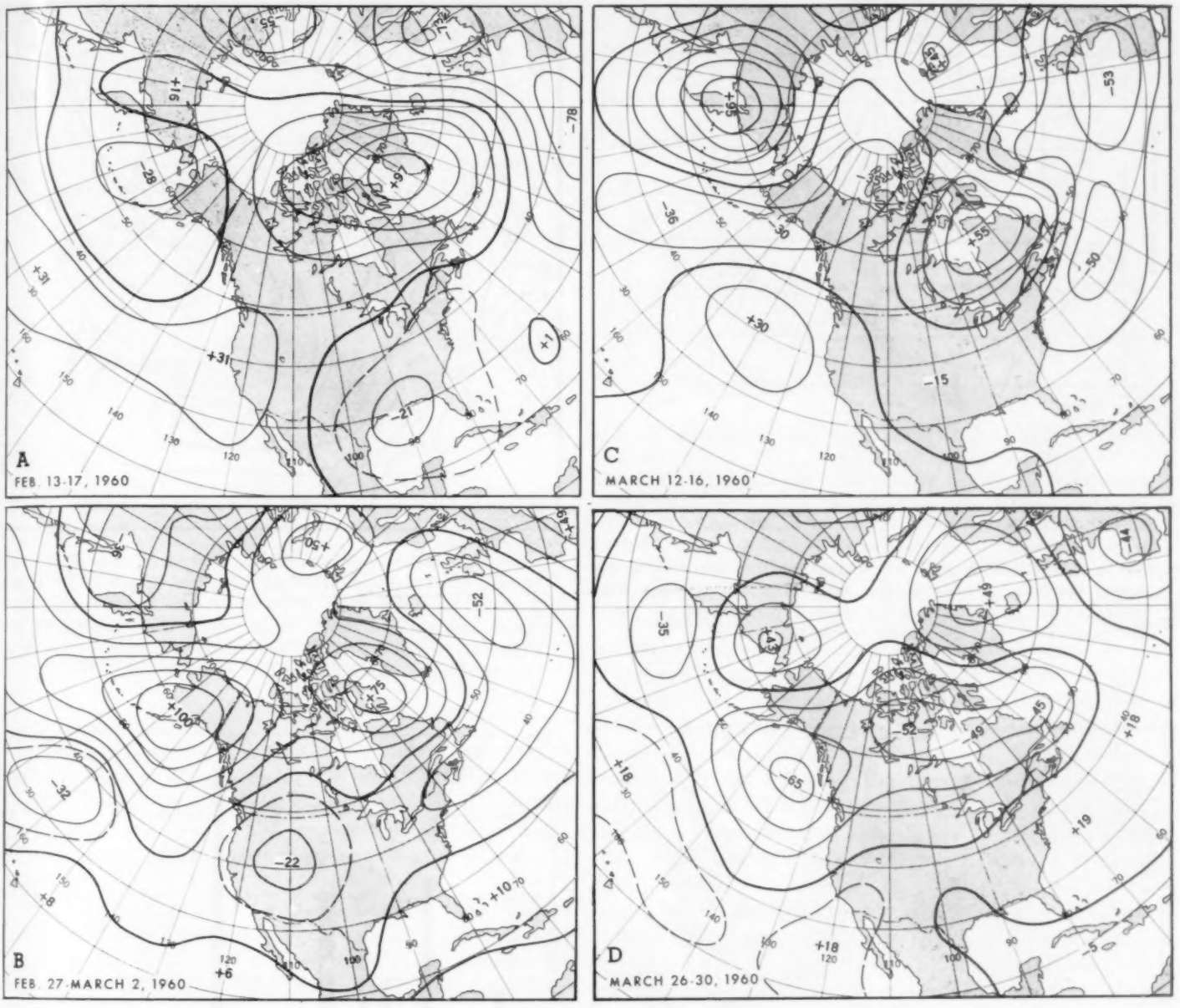

FIGURE 4.—Five-day mean 700-mb. height departures from monthly normal in tens of feet for indicated periods (2 weeks apart) in February and March 1960. Blocking surge [6] was significant evolution of circulation.

In the remainder of the country precipitation was subnormal under the influence of dry, northerly flow between the trough in the east and ridge in the west (fig. 1), a pattern favorable for dry weather.

PERIODICITY

Periodic recurrences in the weather have been noted by several investigators [1, 2, 7]. As pointed out by Namias [7], periodicities frequently occur in spring and also are probably most apparent during periods of persistent or slowly changing general circulations, such as existed this March. During such periods several storms frequently pursue the same general track. This March both layman and meteorologist in Washington, D.C., commented on the fact that storms were affecting the area every Thursday. A plot against time of the total precipitation for each day (fig. 8) shows an approximately 7-day periodicity in February which maintained remarkably well throughout most of March. It is interesting to note that a trace was reported on March 24, the expected time for precipitation if the cycle had continued, even though marked changes in the mean circulation had occurred by this time.

TEMPERATURE

The outstanding weather feature of March 1960 was the extreme and tenacious cold over a large area of the eastern United States. The March mean temperatures were the lowest on record this year at a great many stations (fig. 9).

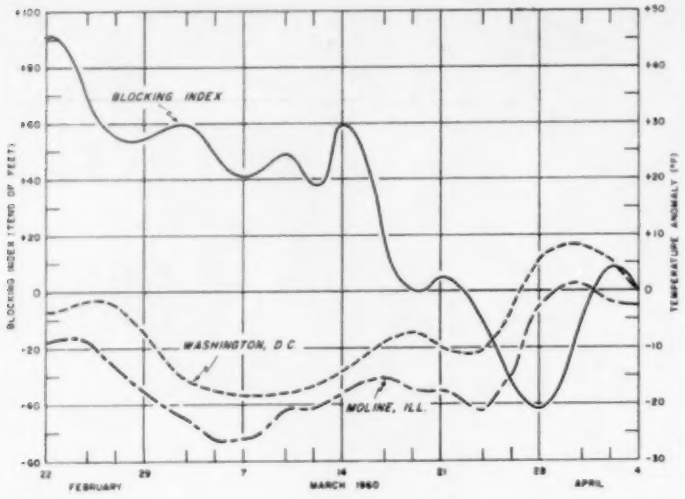

FIGURE 5.—Time variation of the 5-day mean temperature anomaly (° F.) at Moline, Ill., and Washington, D.C., and the blocking index for February and March 1960. Blocking index is obtained by subtracting the average of the four 5-day mean height anomalies at 40°N., 60°W.; 40°N., 70°W.; 30°N., 60°W.; 30°N., 70°W. from the average of the four at 65°N., 55°W.; 65°N., 75°W.; 55°N., 55°W.; 55°N., 75°W. Large positive value indicates strong blocking. Both blocking and temperature values were computed for all available 5-day mean periods, three per week, and plotted opposite the middle day of the periods.

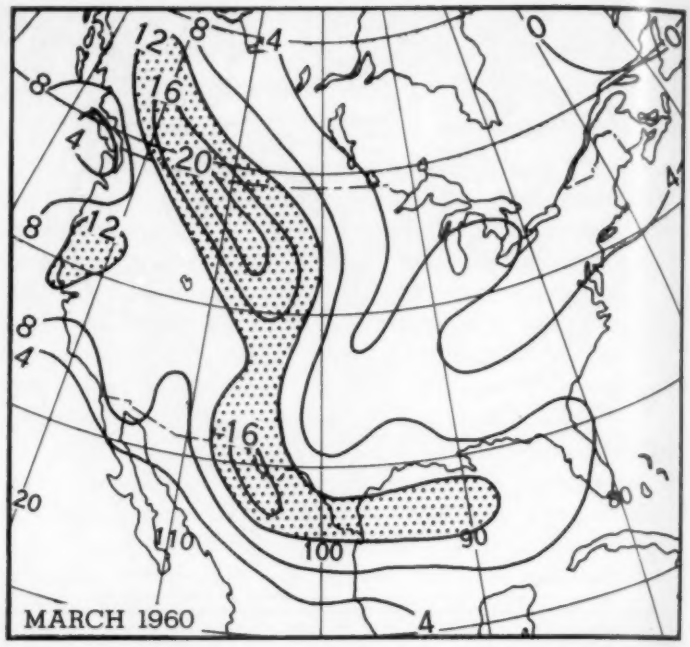

FIGURE 7.—Number of days in March 1960 with fronts of any type (within equal area quadrilaterals of 66,000 n. mi²). All frontal positions are taken from *Daily Weather Map*, 1:00 a.m. EST. Isoline interval is 4 days. Areas with 12 or more days with fronts are stippled Fronts were frequently located far south over the Gulf of Mexico.

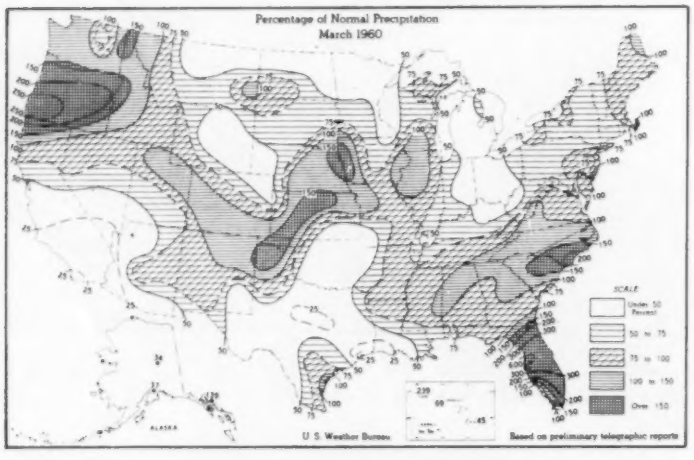

FIGURE 6.—Percentage of normal precipitation for March 1960. Precipitation was abnormally heavy in Oregon, Central Plains, and the Southeast. (From [13] April 11, 1960).

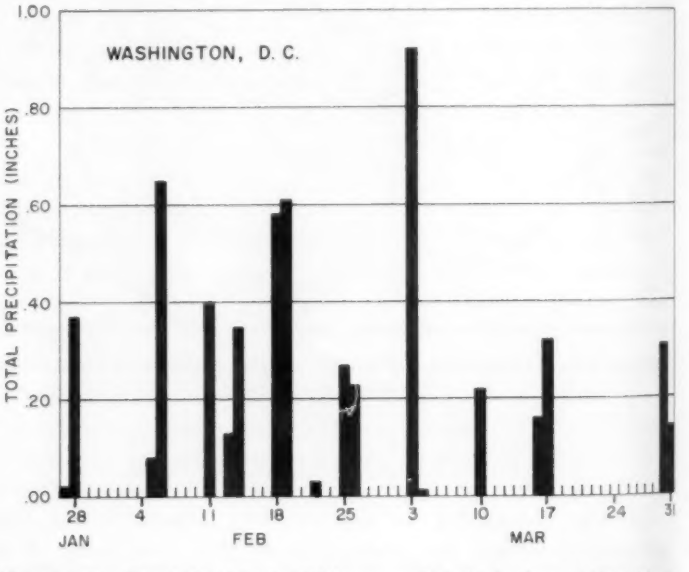

FIGURE 8.—Precipitation for 24-hour periods in inches at Washington, D.C., for February 27–March 31, 1960. Interesting 7-day periodicity existed from mid-February to mid-March.

Some old records were broken by a wide margin. For example, at Moline, Ill., the March mean temperature of 19.9° F. was 7.3° below the previous record made in 1912. Also, this March was the coldest month of the winter at Charleston, W. Va., Louisville, Ky., Harrisburg, Pa., and Dayton, Ohio.

The degree of unusualness of the cold weather may be derived from figure 10 which gives the geographical distribution of the standardized departure from normal of the monthly mean temperature. It was obtained for 130 stations, evenly distributed over the United States, by dividing the observed monthly mean temperature anomalies by their respective standard deviations, which have been computed by Thom [11]. The departures this March were more than 2 standard deviations over a large area of eastern United States, roughly corresponding to the region

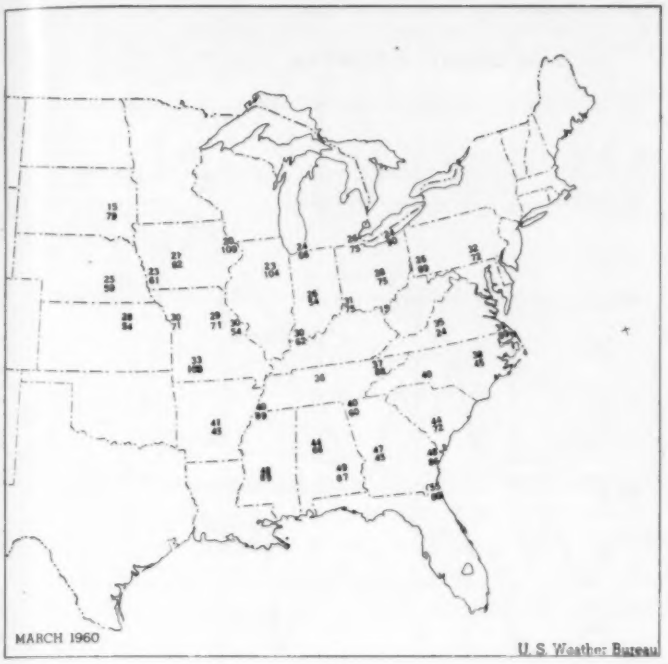

FIGURE 9.—Numbers above stations are mean temperatures (° F.) for March 1960 that were lowest on record for March. Numbers below stations are approximate period of record. These are not all the stations that reported records but were selected to indicate the extensive area of extreme cold.

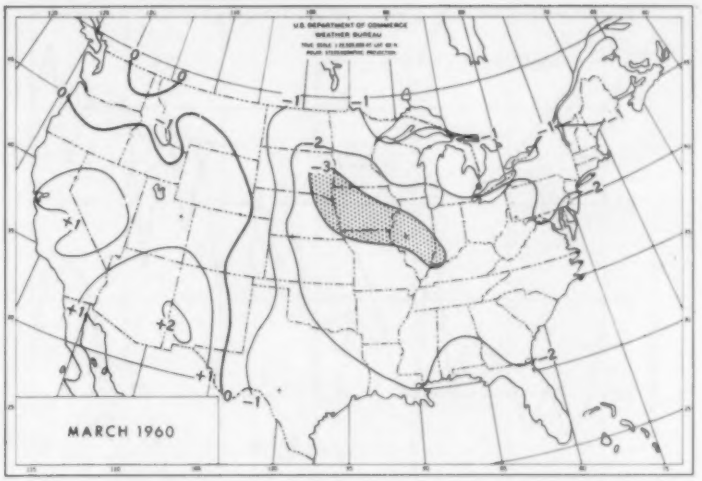

FIGURE 10.—Standardized departures from normal of monthly mean temperatures for March 1960. Average temperatures over a large area in eastern United States were more than 2 standard deviations below normal.

where record temperatures for March occurred, and greater than 3 standard deviations for a sizable region in central United States. With random sampling from a normally distributed population, the probability of obtaining a negative, standardized departure of 3 would be about 1 in 800.

The low monthly mean temperature in the East resulted from persistent extremes. The band of high frequency of fronts (fig. 7) outlines the periphery of the persistently cold area. Frontal systems seldom penetrated the cold air mass that lay over the eastern United States. During the first week most places were colder than normal except for small areas in extreme southwestern and northeastern United States. (See Chart A in No. 10 of [13].) Temperatures averaged more than 25° F. below normal in the northern Rocky Mountain and central Plains States. As the month progressed and ridging took place in the West, the relatively warm area initially confined to the Southwest migrated slowly northward and then spread eastward. In the East the weather in New England cooled markedly, as the 700-mb. trough off the east coast intensified.

For the week ending on March 27, temperatures averaged generally above normal west of the Plains States but were still below normal in the eastern half of the country. Near the end of March temperatures went to above normal over almost the entire United States as the blocking regime disappeared and strong westerlies and warm air spread across the country.

A further breakdown of the temperature records into shorter periods highlights the continuous nature of the cold weather. At Moline, Ill., Washington, D.C., Macon, Ga., and Shreveport, La., representative of the region of extreme cold, the daily maximum and minimum temperatures for March 1960 were plotted against time along with their normal values (fig. 11). During the first part of March both maximum and minimum temperatures remained below their respective normals. In fact, the maximum hovered close to the normal minimum. Many stations reported interesting cold weather phenomena indicating long duration of cold. For example, Atlanta, Ga., had freezing temperatures on 18 days, 7 more than the previous record; at Des Moines, Iowa, temperatures were 10° or more below normal for the first 26 days of March. At the two southern stations, Macon, Ga., and Shreveport, La., warming during the month was rather gradual but greater than the normal, for this time of year, so that by the last week of March, temperatures were near normal. At the northern stations, Moline, Ill., and Washington, D.C., temperatures remained cold until around March 25, 1960, when a pronounced warming set in and temperatures rose rapidly to above normal values. This occurred just after the marked change in circulation described earlier.

5. RELATIONSHIP BETWEEN TEMPERATURE AND CIRCULATION

The above normal ridge in the West and stronger than normal trough in the East fit the observed temperature distribution, but the Gulf of Alaska Low and absence of positive height anomalies in northwestern Canada do not generally favor cold weather in eastern United States [3, 5]. However, Rex [9] showed that in Europe and the Atlantic blocking is associated with cool weather south of the anticyclonic portion of the block. That a similar

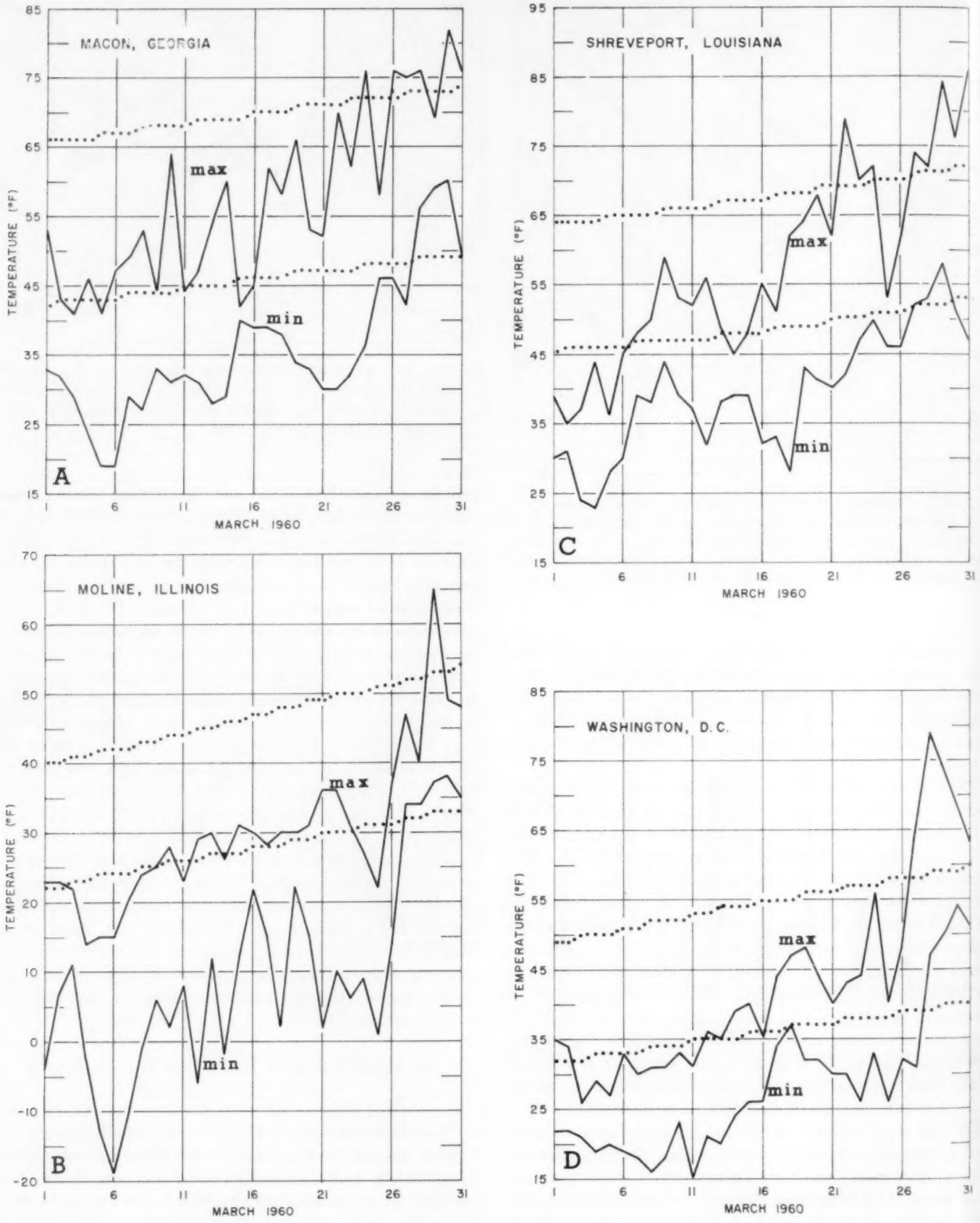

FIGURE 11.—Maximum and minimum surface temperatures (° F.), March normal dotted, March 1960, solid, for indicated cities in eastern United States. Remarkably persistent cold weather existed up to the final days of March.

TABLE 2.—*Snow cover (more than trace) at two stations for selected days in March. Column 3 shows number of years snow cover was present on date in column 2. Column 4 gives depth of snow on the ground on that date in March 1960.*

1 Station	2 Date in March	3 No. of years snow cover present	4 Snow depth March 1960 (in.)
Bismarck, N. Dak. (1943–59)	1	14	0
	10	14	5
	20	10	2
St. Louis, Mo. (1929–59)	1	2	3
	10	4	4
	20	0	10

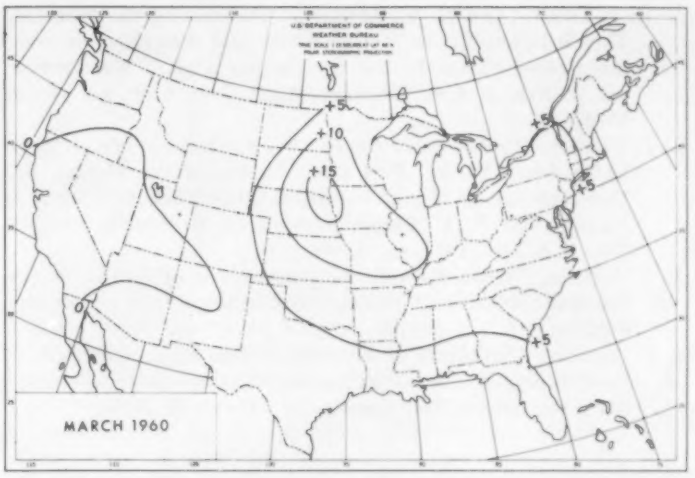

FIGURE 12.—Error (° F.) (forecast minus observed) in temperature specification which was made when statistical prediction equations described in [3] were applied to the observed 30-day mean 700-mb. heights for March 1960. Observed temperatures were much colder in central United States than those indicated by equations.

relationship was operating this March in North America is illustrated in figure 5. Note that while the blocking was strong, temperatures in eastern United States, represented by Moline, Ill., and Washington, D.C., were cold and did not exceed the normal until after the blocking disappeared.

A factor which contributed to the cold temperatures in the United States was the abnormal cold of the air masses leaving the Canadian source region. Monthly mean surface temperatures and thicknesses (1000–700 mb.) averaged below normal everywhere in Canada except along the coasts. Temperatures for the month averaged up to 8° F. below normal and thicknesses 240 ft. below normal in the MacKenzie River Basin. From this area several migratory Arctic anticyclones moved into eastern United States. (See Chart IX in [12] and fig. 2.)

This factor, plus the circulation at 700 mb., although favorable for cool weather, hardly explain the record cold observed this March. It has been suggested by Namias [8] that an important part of the reason for the persistence of such extreme temperatures was the establishment, in the latter part of February, of an extensive and deep snow cover over areas where snow in not normally found at this time of year. He showed that observed temperature anomalies exceeded those normally expected from the observed 700-mb. mean circulation. The direct influence of the circulation on the temperature distribution was assessed objectively, although imperfectly, by using statistical equations developed by Klein et al. [3]. These equations, although designed for 5-day forecasting, were found to explain 63 percent of the temperature variability when applied to observed monthly mean 700-mb. height [3]. The objective temperatures derived in this manner from the observed 700-mb. mean for March 1960 were much too warm in eastern United States where observed temperatures were very cold (fig. 12). This appears to support the hypothesis that snow cover played an important role in keeping the polar outbreaks very cold as they progressed southward.

Charts prepared at the National Meteorological Center of the U.S. Weather Bureau showed that the southern boundary of the snow cover (1 inch or more) extended roughly on March 1, from southern New England to the Texas Panhandle, on March 10, from South Carolina to Colorado, and on March 20, from southern New England to Kansas.

At many stations with long periods of record daily values of the depth of snow on the ground are available, although homogeneous records are scarce. Nevertheless, the records at Bismarck, N. Dak. and St. Louis, Mo., were examined to help estimate the normal frequency of snow cover in and upstream from the area of extreme cold this March. The results are presented along with the snow cover for March 1960 in table 2. These data indicate that snow cover is quite common at Bismarck in March but rather rare at St. Louis. This, in conjunction with the U.S. Weather Bureau snow cover chart previously referred to, suggests that the southern boundary of snow cover extended farther south than normal this March. This factor could have contributed significantly to the excessively cold temperatures, especially in the southern areas.

REFERENCES

1. G. W. Brier, "Seven Day Periodicities in Certain Meteorological Parameters During the Period 1899–1951," *Bulletin of the American Meteorological Society*, vol. 36, No. 6, June 1955, pp. 265–277.
2. H. F. Hawkins, Jr., "The Weather and Circulation of March 1954–A Cool March with a 6-day Periodicity," *Monthly Weather Review*, vol. 82, No. 3, Mar. 1954, pp. 80–86.
3. W. H. Klein, B. M. Lewis, and I. Enger, "Objective Prediction of Five-Day Mean Temperature During Winter," *Journal of Meteorology*, vol. 16, No. 6, Dec. 1959, pp. 672–688.
4. D. M. Ludlum, "The Great Early March Snowstorm of 1960," *Weatherwise*, vol. 13, No. 2, Apr. 1960, pp. 59–62 and 73.

5. D. E. Martin and H. F. Hawkins, "Forecasting the Weather: The Relationship of Temperature and Precipitation over the United States to the Circulation Aloft," *Weatherwise*, vol. 3, Nos. 2, 4, 6, February, April, June 1950, pp. 16–19, 40–43, 65–67.
6. J. Namias, "Problems Suggested by a Synoptic Study of Mean 10,000-foot Charts," Part I of "Studies of the Motion and Development of Long Waves in the Westerlies," by J. Namias and P. F. Clapp, *Journal of Meteorology*, vol. 1, Nos. 3, 4, Dec. 1944, pp. 57–66.
7. J. Namias, "Quasi-Periodic Cyclogenesis in Relation to the General Circulation," *Tellus*, vol. 6, No. 1, Feb. 1954, pp. 8–22.
8. J. Namias, "Problems of Dynamic Climatology Germane to Long Range Weather Forecasting," Lecture given at Florida State University, Tallahassee, Fla., March 24, 1960.
9. D. F. Rex, "Blocking Action in the Middle Troposphere and its Effects upon Regional Climate, II. The Climatology of Blocking Action," *Tellus*, vol. 2, No. 4, Nov. 1950, pp. 275–301.
10. L. P. Stark, "The Weather and Circulation of February 1960—A Cold Stormy Month over the United States Associated with Widespread Blocking," *Monthly Weather Review*, vol. 88, No. 2, Feb. 1960, pp. 72–78.
11. H. C. S. Thom, Standard Deviation of Monthly Average Temperature, U.S. Weather Bureau, Manuscript, Washington, D.C., 1955, 12 pp.
12. U.S. Weather Bureau, *Climatological Data, National Summary*, vol. 11, No. 3, March 1960.
13. U.S. Weather Bureau, *Weekly Weather and Crop Bulletin, National Summary*, vol. XLVII, Nos. 10–15, March 7, 14, 21, 28, and April 4, 11, 1960.

Publications by Weather Bureau Authors

G. L. BARGER, "Review of *An Introduction to Physical Microclimatology*, F. A. Brooks, Univ. of Calif., Davis, Calif.", *Bulletin of the American Meteorological Society*, vol. 41, No. 2, Feb. 1960, pp. 93–95.

FORECASTS AND SYNOPTIC REPORTS DIVISION, "Weather Radio Broadcasts", *Weatherwise*, vol. 12, No. 2, April 1959, pp. 98–103.

S. FRITZ, "On Observing the Atmosphere From Satellites. I. Cloud Observations," *Weatherwise*, vol. 12, No. 4, Aug. 1959, pp. 139–144, 163–165.

F. A. GIFFORD, JR., "Computation of Pollution From Several Sources," [Letter to Editor], *International Journal of Air Pollution*, vol. 2, No. 1, July 1959, pp. 109–110.

F. A. GIFFORD, JR., "Smoke Plumes as Quantitative Air Pollution Indices," *International Journal of Air Pollution*, vol. 2, No. 1, July 1959, pp. 42–50.

F. A. GIFFORD, JR., "Review of *Turbulent Transfer in the Lower Atmosphere* by C. H. B. Priestley, Univ. of Chicago Press, 1959," *Bulletin of the American Meteorological Society*, vol. 41, No. 2, Feb. 1960, pp. 95, 98.

W. H. HAGGARD, "Review of *The Climatological Atlas of the Czechoslovak Republic*, Artia, Prague, Czechoslovakia," *Bulletin of the American Meteorological Society*, vol. 40, No. 11, Nov. 1959, p. 584.

M. N. HUNTER, "A Technique for Processing Teleprinter Copy of Numerical Weather-Prediction Data," *Bulletin of the American Meteorological Society*, vol. 40, No. 7, July 1959, pp. 333–335.

W. H. KLEIN, "The Circulation and Weather of 1959," *Weatherwise*, vol. 13, No. 1, Feb. 1960, pp. 7–14.

W. H. KLEIN, B. LEWIS, AND I. ENGER, "Objective Prediction of Five-Day Mean Temperatures During Winter," *Journal of Meteorology*, vol. 16, No. 6, Dec. 1959, pp. 672–682.

P. H. KUTSCHENREUTER, "A Study of the Effect of Weather on Mortality," *Transactions* of New York Academy of Sciences, Series II, vol. 22, No. 2, Dec. 1959, pp. 126–138.

H. E. LANDSBERG, "Facets of Climate," *The Science Teacher*, vol. 27, No. 2, 1960, pp. 6–12.

H. E. LANDSBERG, "Review, *Physikalische Dynamik der Atmosphäre*, A. and F. Defant, Akademische Verlagsgesellschaft Frankfurt am Main, 1958," *Transactions* of the American Geophysical Union, vol. 40, No. 2, June 1959, p. 123.

H. E. LANDSBERG, "Review of *Recent Research in Climatology*, Harmon Craig, Editor, Univ. of Calif., Research in Water Resources, La Jolla, 1958," *Bulletin of the American Meteorological Society*. vol. 39, No. 8, Aug. 1958, p. 454.

N. LIEURANCE, "Meteorological Service for Merchant Shipping," WMO *Technical Note*, No. 23, Lectures at Commission on Maritime Meteorology, Second Session, Oct. 1956, Geneva, 1958.

R. A. MCCORMICK (co-author), "The Spectrum of Vertical Velocity Near the Ground," Institute of Aero Science, *Report* 59–6, 1959.

L. MACHTA, "Air Pollution and Radioactivity Circulation Problems," *Proceedings of the National Academy of Sciences*, vol. 45, No. 12, Dec. 1959, pp. 1672–1686.

L. MACHTA, Letter to editor, *Scientific American*, vol. 201, No. 5, Nov. 1959, pp. 16–17.

L. MACHTA AND K. M. NAGLER, "Meteorology—Fallout and Weathering," *Symposium—The Shorter-Term Biological Hazards of a Fallout Field*, Washington, D.C., Dec. 12–14, 1956, U.S. Atomic Energy Commission and Department of Defense, 1958.

B. I. MILLER AND P. L. MOORE, "A Comparison of Hurricane Steering Levels," *Bulletin of the American Meteorological Society*, vol. 41, No. 2, Feb. 1960, pp. 59–63.

F. W. REICHELDERFER, "Modernizing Our National Aviation Weather System," *Sperryscope*, Fourth Quarter 1958, vol. 14, No. 11, pp. 12–16.

V. D. ROCKNEY, "New Developments in Observations and Instrumentation in the Weather Bureau," *Bulletin of the American Meteorological Society*, vol. 40, No. 11, Nov. 1959, pp. 554–560.

M. J. SCHROEDER [with C. M. COUNTRYMAN], "Prescribed Burn Fireclimate Survey 1–57, 2–57, 3–57, 4–57," California Forest and Range Experiment Station, *Technical Paper*, Nos. 29, 31, 34, 35, Dec. 1958–July 1959.

H. C. S. THOM, "Distribution of Annual Tropical Cyclone Frequency," *Journal of Geophysical Research*, vol. 65, No. 1, Jan. 1960, pp. 213–222.

H. C. S. THOM, "A Time Interval Distribution for Excessive Rainfall," *Proceedings of the American Society of Civil Engineers* [Separate No. 2083], July 1959.

J. C. THOMPSON, "Review, *Introduction to Meteorology*, Sverre Petterssen, 2nd edition, McGraw-Hill, New York 1958," *Bulletin of the American Meteorological Society*, vol. 39, No. 12, Dec. 1958, p. 660.

D. Q. WARK, "Review of *Dictionary of Astronomy and Astronautics*, Spitz and Gaynor, Philosophical Library, Inc., New York, 1959," *Bulletin of the American Meteorological Society*, vol. 40, No. 12, Dec. 1959, p. 640.

H. WEXLER, "The 'Kernlose' Winter in Antarctica," *Geophysica*, vol. 6, Nos. 3–4, 1959, pp. 577–595.

H. WEXLER, "Seasonal and Other Temperature Changes in the Antarctic Atmosphere," *Quarterly Journal of the Royal Meteorological Society*, vol. 85, No. 365, July 1959, pp. 196–208.

H. WEXLER, "A Warming Trend at Little America, Antarctica," *Weather*, vol. 14, No. 6, 1959, pp. 191–197.

H. WEXLER, "Review of *Meteorology of the Antarctic*, M. P. van Rooy editor, Weather Bureau, Dept. of Transport, Pretoria, South Africa, 1957," *Bulletin of the American Meteorological Society*, vol. 39, No. 9, Sept. 1958, pp. 505–507.

Publication of Weather Notes

Many years ago the *Monthly Weather Review* published detailed eyewitness accounts of exceptional storms. These accounts both enrich the meteorologist's knowledge of storms and provide him with particular details that cannot be found elsewhere. Because such information bears directly upon questions the meteorologist must attempt to answer about weather phenomena (for example, the identification of storms as tornadoes), and because the information has potential value in both the research and service programs of the Weather Bureau, publication of eyewitness accounts and brief analyses of exceptional storms and other meteorological phenomena was resumed in the April 1955 issue. They appear from time to time under the heading "Weather Notes".

Contributions to these "Notes" are invited from readers of the Review. There is no limitation placed on length of description but it is expected that most will be short accounts. Any weather peculiarities, whether storms or other phenomena, are acceptable subject matter. Material should be addressed to Editor, Monthly Weather Review, U.S. Weather Bureau, Washington 25, D.C.

U.S. GOVERNMENT PRINTING OFFICE: 1960